第一章 半导体材料的基本性质与生长技术

曹丙强

2019.09

本章主要参考文献：

《半导体器件的材料物理学基础》（科学出版社）

第一章

主 要 内 容

- 半导体材料的基本性质
- 半导体材料的种类
- 半导体材料的生长技术
- 半导体材料的用途

一、半导体的基本性质

- 固体材料的导电性（电阻），可分成：
  - 超导体、导体、半导体、（拓扑绝缘体）、绝缘体

- 电阻率
  - 导体： $\rho < 10^{-4}\Omega cm$　　例如：$\rho_{Cu}=10^{-6}\Omega cm$
  - 半导体：$10^{-3}\Omega cm < \rho < 10^{8}\Omega cm$　　$\rho_{Ge}=0.2\Omega cm$
  - 绝缘体：$\rho > 10^{8}\Omega cm$

导体、半导体和绝缘体的电阻率范围

材料	导体	半导体	绝缘体
电阻率ρ(Ω cm)	$< 10^{-3}$	$10^{-3}\sim10^{9}$	$>10^{9}$

半导体材料的基本性质

【1】主要依赖于掺杂的产生的不同载流子

- 金属的导电性：大量的自由电子

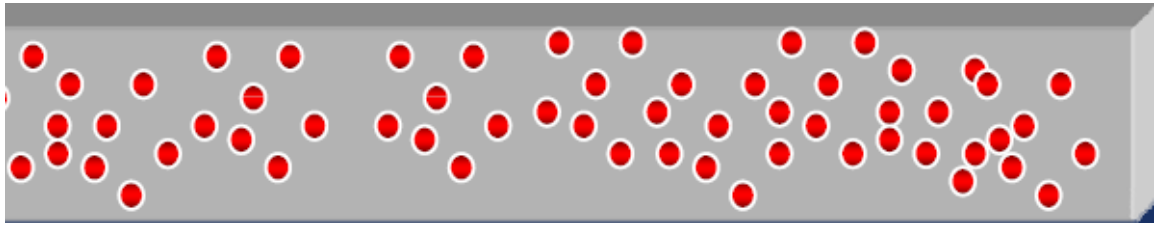

- 半导体的导电性：
  - ➢ 依靠可以移动的电子或空穴（载流子）

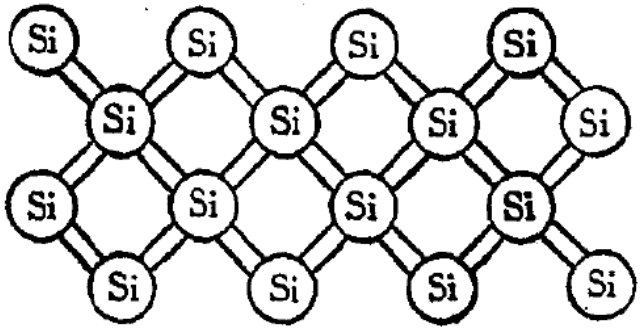

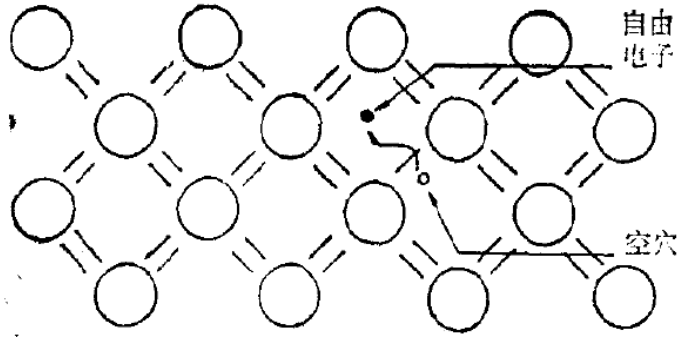

依靠光照或者晶体本身内在的原子热运动，电子可以摆脱共价键的束缚，进而产生可以自由移动的电子和空穴，但是浓度很小（$<1.5\times10^{10}/cm^3$），对半导体的导电性影响不大。

半导体材料的基本性质

【2】可调导电性（载流子浓度的变化）

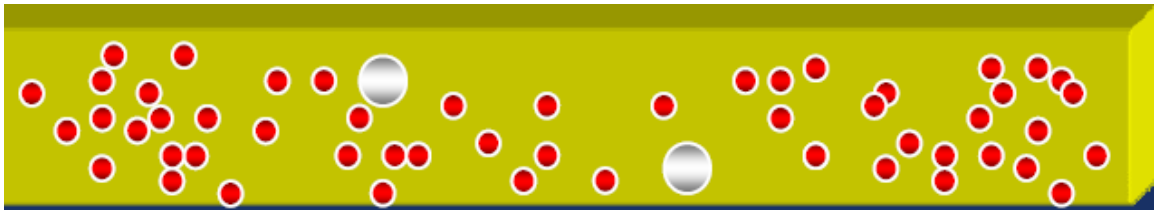

N-型半导体，电子导电，施主掺杂

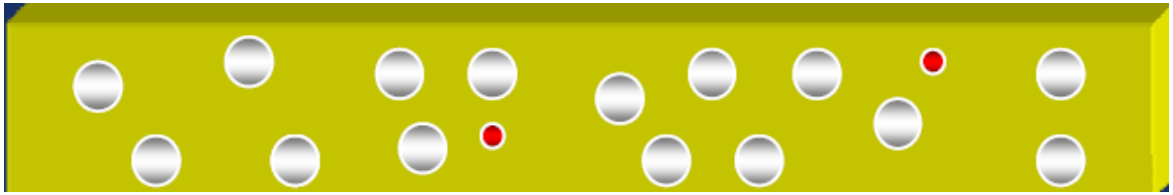

P-型半导体，空穴导电，受主掺杂

比如：❖ 温度升高使半导体导电能力增强，电阻率下降

如室温附近的纯硅(Si)，温度每增加8℃，电阻率相应地降低50%左右

❖ 微量杂质含量可以显著改变半导体的导电能力

以纯硅中每100万个硅原子掺进一个Ⅴ族杂质（比如磷）为例，这时硅的纯度仍高达99.9999%，但电阻率在室温下却由大约214,000Ω cm降至0.2Ω cm以下

➢ 其他典型性质

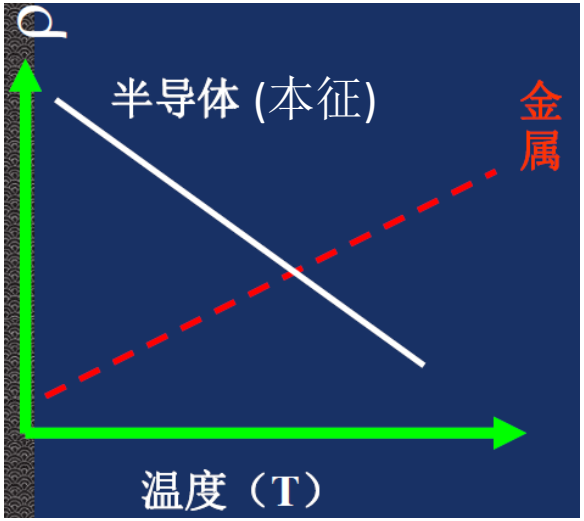

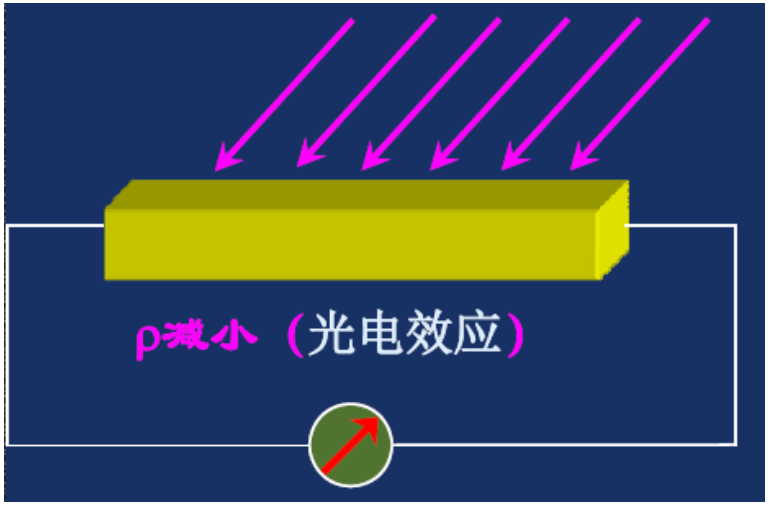

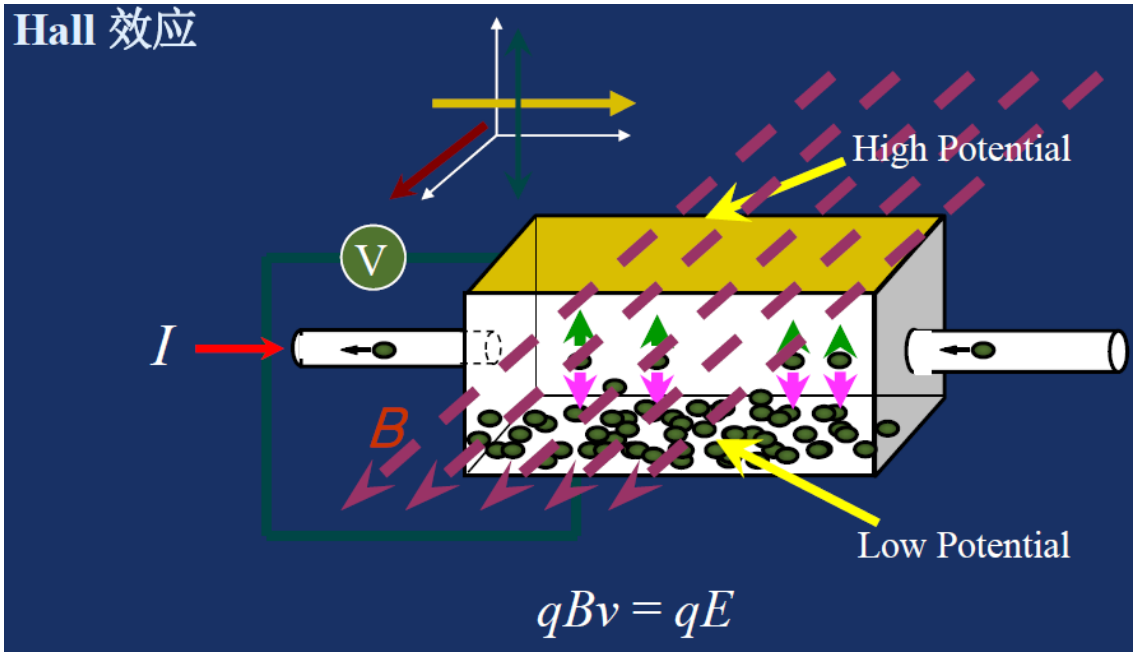

量子霍尔效应家族

拓扑绝缘体/topological insulator;

- 体是绝缘体；表面是导体的一类特殊材料

  HgTe量子阱；Bi_xSe_y家族材料（ Bi_xSe_y， Bi_xTe_y， Sb_xSe_y ）

- 典型特征

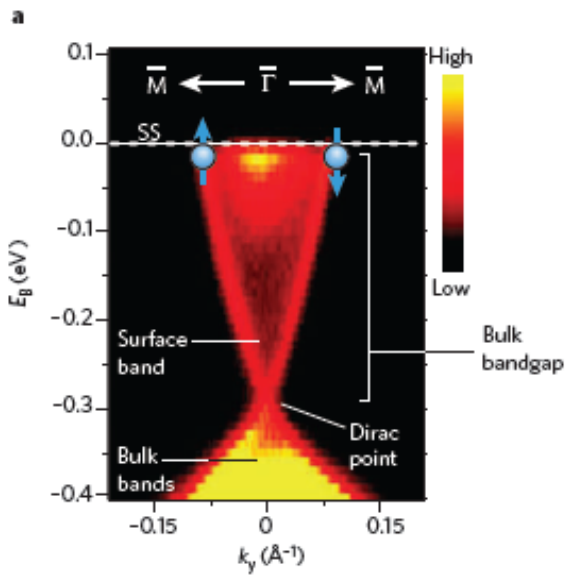

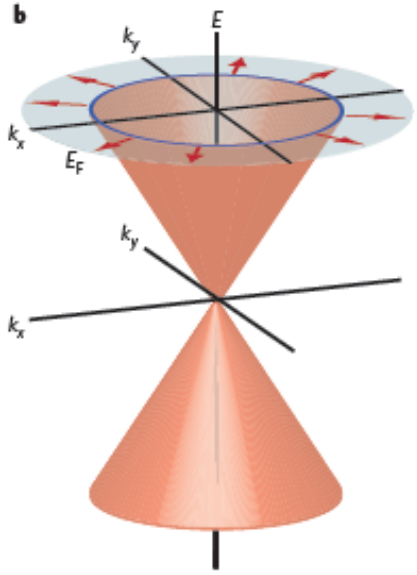

Figure 3 | Signatures of the exotic metallic surface states in topological insulators. **a**, The electronic structure of Bi_2Se_3, as measured by ARPES. Measured energy electron energy, E_B, is plotted against electron momentum, k_y. High intensity (red and yellow areas) indicates a non-zero electronic density of states. The surface bands crossing the bulk bandgap enclose a single Dirac point at the Brillouin-zone centre ($\bar{\Gamma}$), which is the signature that this material is a topological insulator. $\bar{M}$ indicates the centre of an edge of the Brillouin zone, and the path in the Brillouin zone is indicated by white arrows. The direction of electron spin is indicated by blue arrows. (Panel modified, with permission, from ref. 12; data taken from refs 12 and 23.) **b**, Theoretical idealization of the electronic structure of Bi_2Se_3, showing the rotation of the spin degree of freedom (red arrows) as an electron (with energy E) moves around the Fermi surface (with Fermi energy E_F). Scattering of the surface electrons by non-magnetic disorder will modify the details of the electronic wavefunctions but will not eliminate the metallic surface.

Joel E. Moore， Nature（2010）

Hall Effect	1879	Anomalous Hall Effect	1880
Integer QHE	1980	QAHE?	
Fractional QHE	1982		

QHE under a magnetic field

QHE without a magnetic field

影响应用的一个问题：强磁场

量子霍尔效应：十万高斯

地磁场：0.5高斯

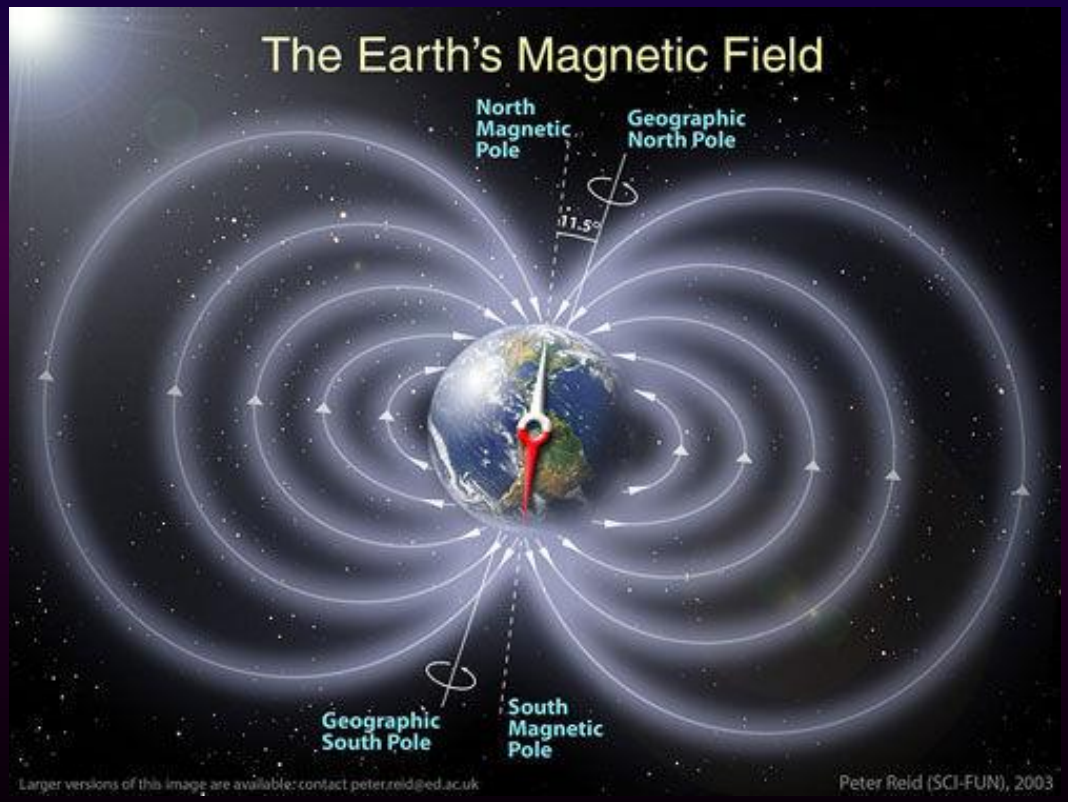

Science

REPORTS

Experimental Observation of the Quantum Anomalous Hall Effect in a Magnetic Topological Insulator

Cui-Zu Chang,[1,2]* Jinsong Zhang,[1]* Xiao Feng,[1,2]* Jie Shen,[2]* Zuocheng Zhang,[1] Minghua Guo,[1] Kang Li,[2] Yunbo Ou,[2] Pang Wei,[2] Li-Li Wang,[2] Zhong-Qing Ji,[2] Yang Feng,[1] Shuaihua Ji,[1] Xi Chen,[1] Jinfeng Jia,[1] Xi Dai,[2] Zhong Fang,[2] Shou-Cheng Zhang,[3] Ke He,[2]† Yayu Wang,[1]† Li Lu,[2] Xu-Cun Ma,[2] Qi-Kun Xue[1]†

The quantized version of the anomalous Hall effect has been predicted to occur in magnetic topological insulators, but the experimental realization has been challenging. Here, we report the observation of the quantum anomalous Hall (QAH) effect in thin films of chromium-doped $(Bi,Sb)_2Te_3$, a magnetic topological insulator. At zero magnetic field, the gate-tuned anomalous Hall resistance reaches the predicted quantized value of h/e^2, accompanied by a considerable drop in the longitudinal resistance. Under a strong magnetic field, the longitudinal resistance vanishes, whereas the Hall resistance remains at the quantized value. The realization of the QAH effect may lead to the development of low-power-consumption electronics.

The quantum Hall effect (QHE), a quantized version of the Hall effect (*1*), was observed in two-dimensional (2D) electron systems more than 30 years ago (*2*, *3*). In QHE, the Hall resistance, which is the voltage across the transverse direction of a conductor divided by the longitudinal current, is quantized into plateaus of height $h/\nu e^2$, with h being Planck's constant, e the electron's charge, and ν an integer (*2*) or a certain fraction (*3*). In these systems, the QHE is a consequence of the formation of well-defined Landau levels and thus only possible in high-mobility samples and strong external magnetic fields. However, there have been numerous proposals to realize the QHE without applying any magnetic field (*4*–*11*). Among these proposals, using the thin film of a magnetic topological insulator (TI) (*6*–*9*, *11*), a new class of quantum matter discovered recently (*12*, *13*), is one of the most promising routes.

Magnetic field–induced Landau quantization drives a 2D electron system into an insulating phase that is topologically different from the vacuum (*14*, *15*); as a consequence, dissipationless states appear at sample edges. The topologically nontrivial electronic structure can also occur in certain 2D insulators with time reversal symmetry (TRS) broken by current loops (*4*) or by magnetic ordering (*6*), requiring neither Landau

[1]State Key Laboratory of Low-Dimensional Quantum Physics, Department of Physics, Tsinghua University, Beijing 100084, China. [2]Beijing National Laboratory for Condensed Matter Physics, Institute of Physics, The Chinese Academy of Sciences, Beijing 100190, China. [3]Department of Physics, Stanford University, Stanford, CA 94305–4045, USA.

*These authors contributed equally to this work.
†Corresponding author. E-mail: qkxue@mail.tsinghua.edu.cn (Q.-K.X.); kehe@iphy.ac.cn (K.H.); yayuwang@tsinghua.edu.cn (Y.W.)

Quantized AHE !

experiment

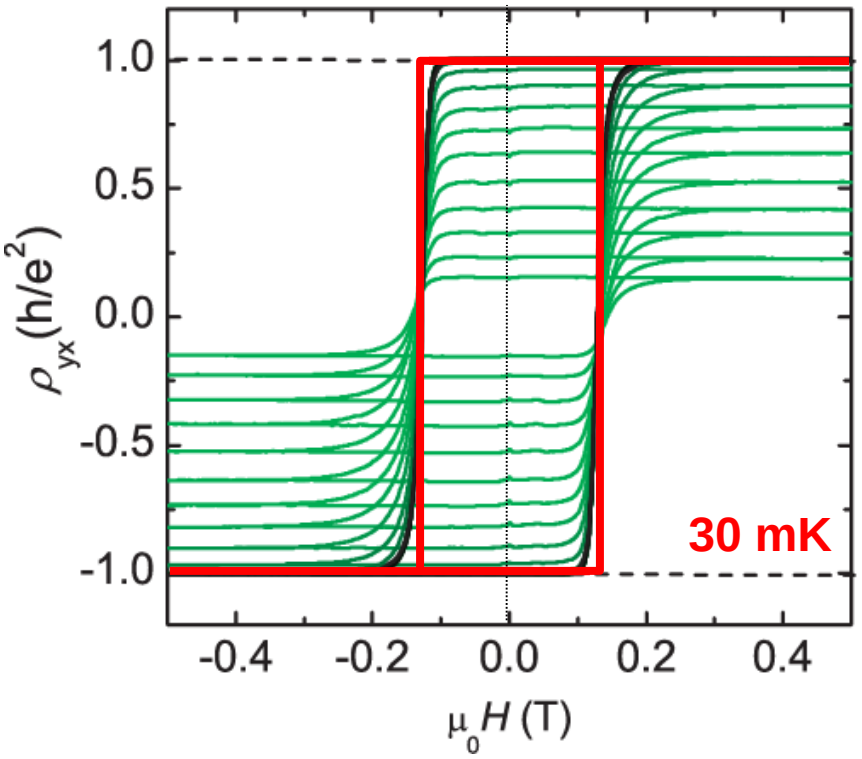

theory

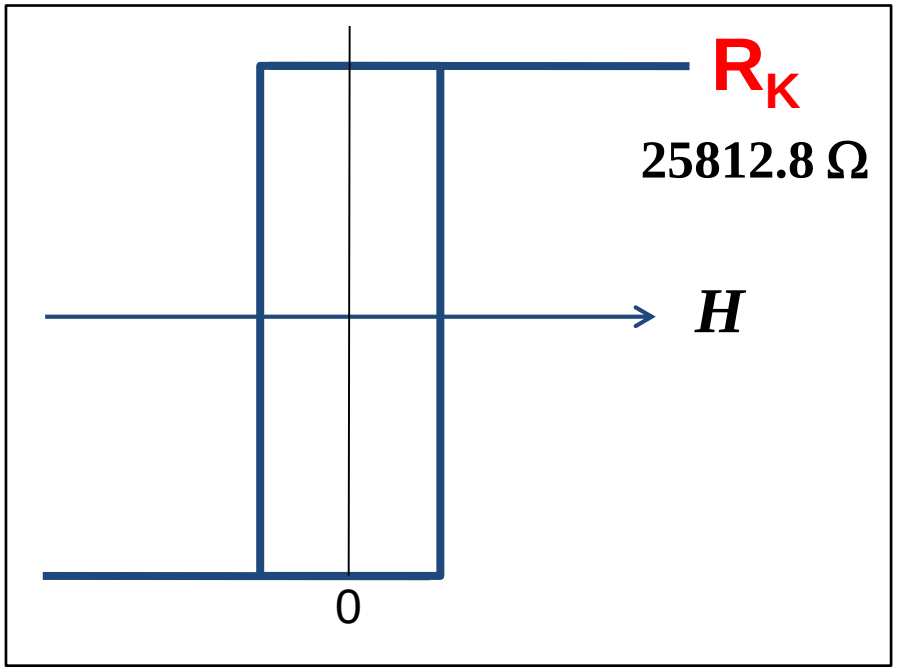

Prof. Li Lu (IOP)

- 20 samples at T = 1.5 K
- 6 samples at T = 90 mK (zero-field Hall resistance: 0.87 to 0.98 h/e^2)
- 2 samples at T = 30 mK (full quantization at h/e^2)

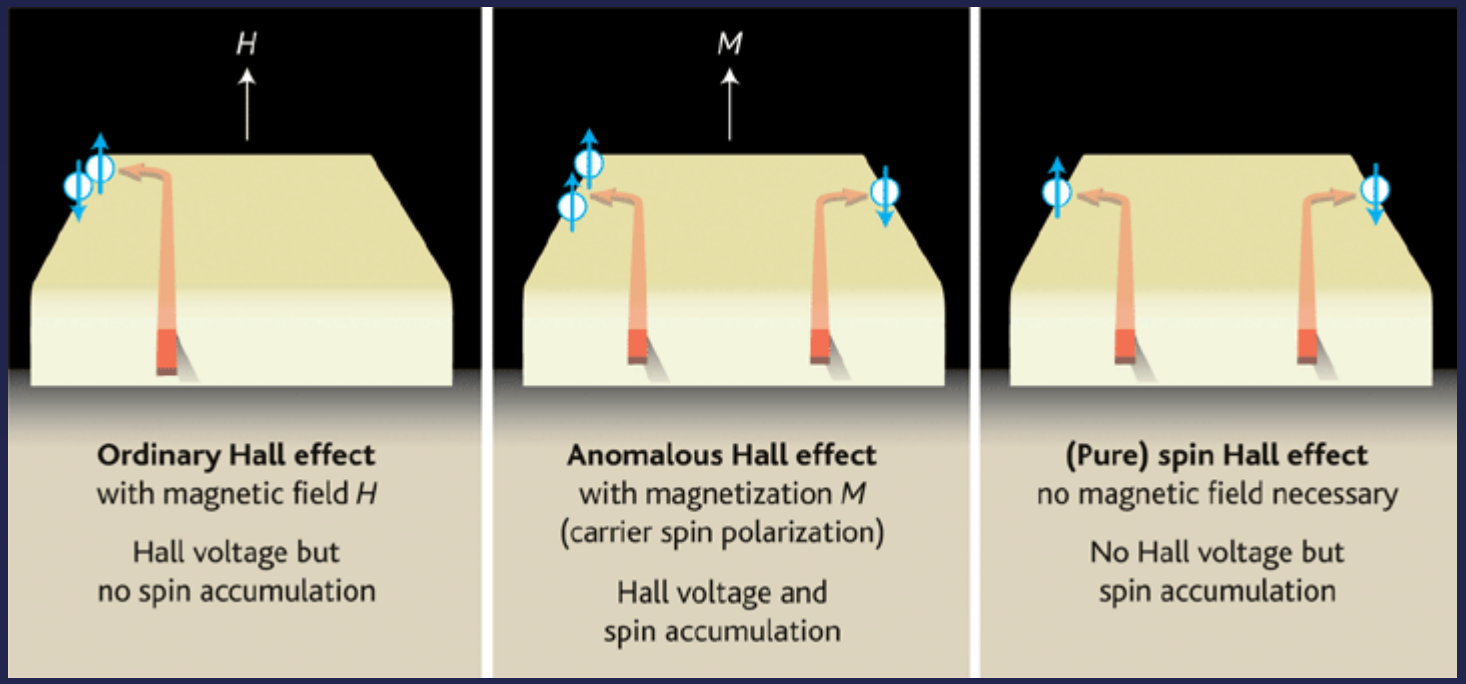

Junichiro et al., Science, 2005

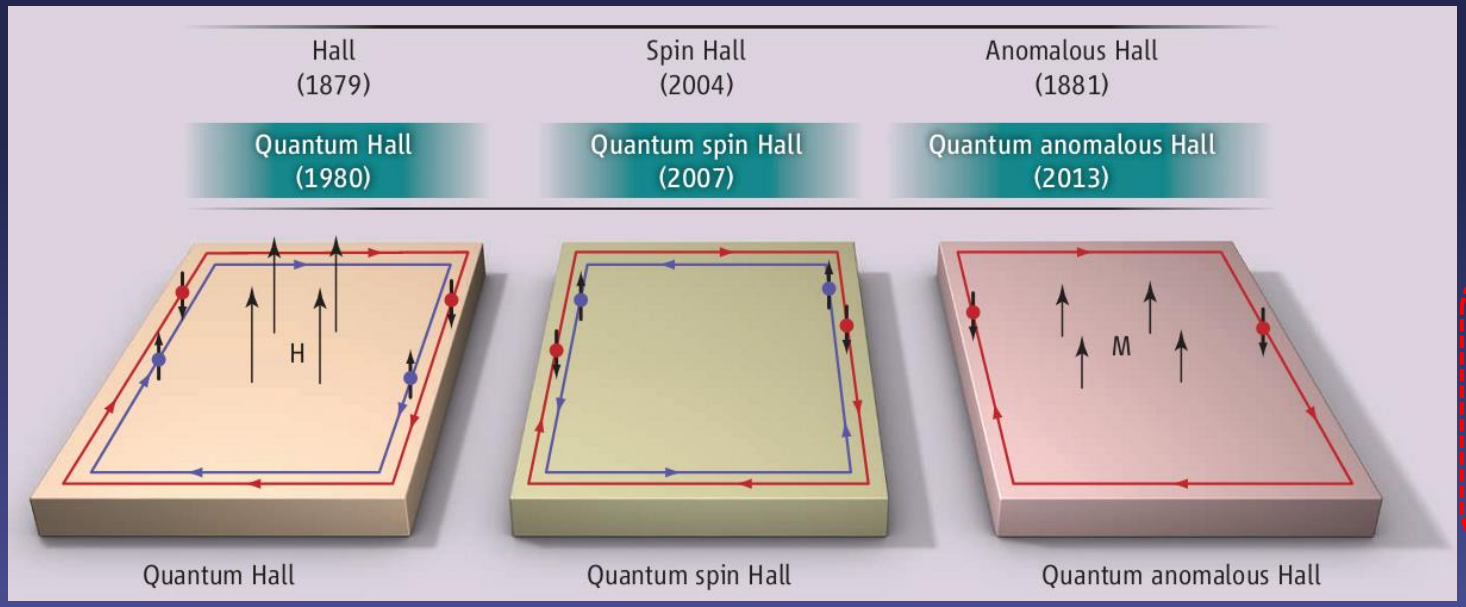

Seongshik Oh, Science, 2013

5QL Cr-doped $(Bi,Sb)_2Te_3$ films

The Nobel Prize in Physics 2016

David J. Thouless, F. Duncan M. Haldane, J. Michael Kosterlitz

Share this: 1.5K

The Nobel Prize in Physics 2016

© Trinity Hall, Cambridge University. Photo: Kiloran Howard

David J. Thouless

Prize share: 1/2

Photo: Princeton University, Comms. Office, D. Applewhite

F. Duncan M. Haldane

Prize share: 1/4

Ill: N. Elmehed. © Nobel Media 2016

J. Michael Kosterlitz

Prize share: 1/4

The Nobel Prize in Physics 2016 was divided, one half awarded to David J. Thouless, the other half jointly to F. Duncan M. Haldane and J. Michael Kosterlitz *"for theoretical discoveries of topological phase transitions and topological phases of matter"*.

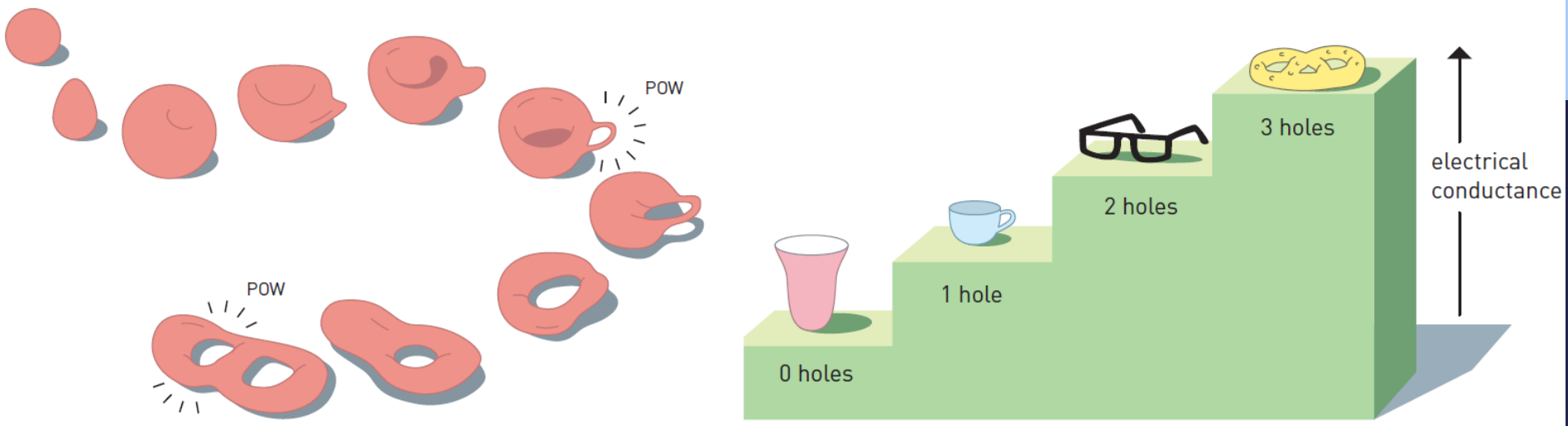

Fig 3. Topology. This branch of mathematics is interested in properties that change step-wise, like the number of holes in the above objects. Topology was the key to the Nobel Laureates' discoveries, and it explains why electrical conductivity inside thin layers changes in integer steps.

Both quantum Hall fluids and even magnetic atomic chains are included in this new group of topological states. Later, researchers discovered several other unexpected topological states of matter, not only in chains and thin border layers, but also in ordinary three-dimensional materials.

Topological insulators, topological superconductors and topological metals are now being talked about. These are examples of areas which, over the last decade, have defined frontline research in condensed matter physics, not least because of the hope that topological materials will be useful for new generations of electronics and superconductors, or in future quantum computers. Current research is now revealing the secrets of matter in the exotic flatlands discovered by this year's Nobel Laureates.

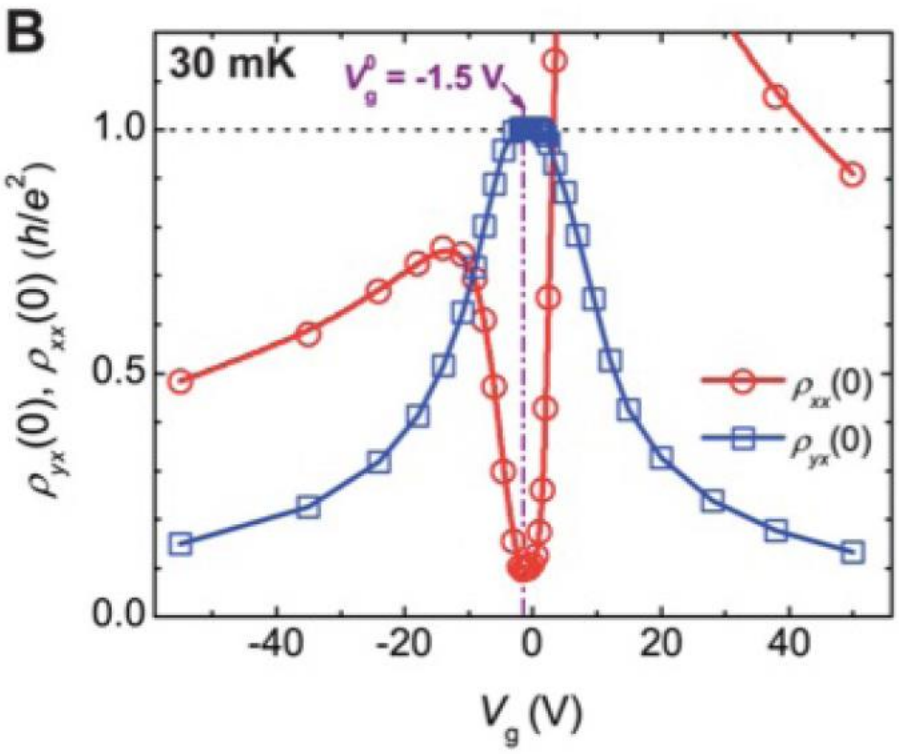

Figure 6: *The blue curve shows the Hall resistance* ρ_{yx} *as a function of the gate voltage at zero magnetic field. Note the plateau at* $V_g = 0$*, which is the point corresponding to a filled band. (Figure from Ref. [15].)*

[15] Cui-Zu Chang, Jinsong Zhang, Xiao Feng, Jie Shen, Zuocheng Zhang, Minghua Guo, Kang Li, Yunbo Ou, Pang Wei, Li-Li Wang, et al. Experimental observation of the quantum anomalous hall effect in a magnetic topological insulator. *Science*, 340(6129):167–170, 2013.

微电子学、集成电路发展的一个瓶颈

目前芯片中的电子

电子运动过程中受到散射：
芯片发热、速度变慢…

50纳米集成电路：
发热占1/3

量子霍尔态的电子

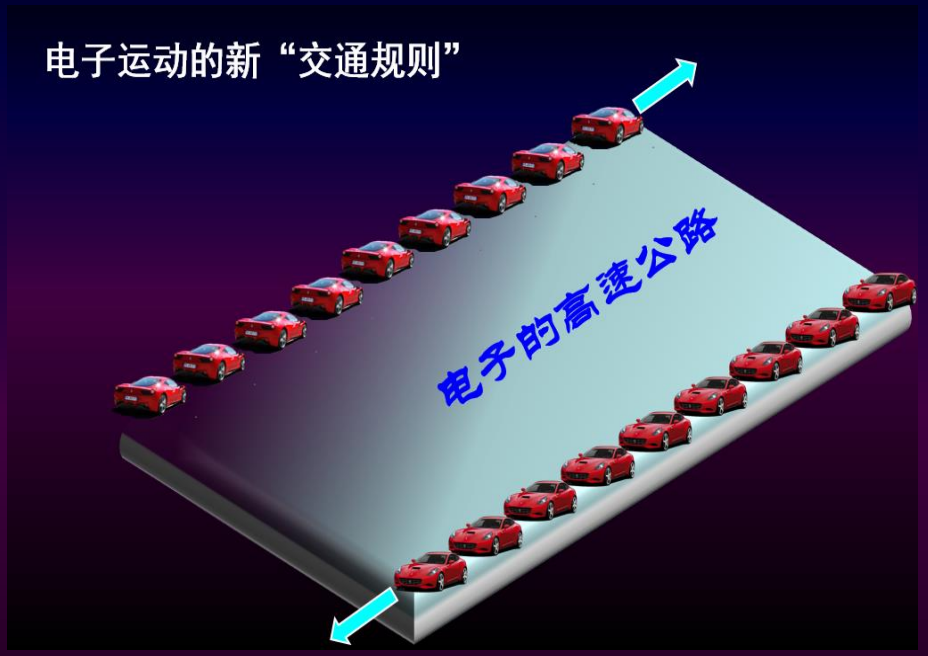

电子的运动制定的交通规则：
只能“一往无前”地前进！

⇨ 极低能耗电子器件

作业（2）

- 查找相关资料，尝试阐明：

  Hall effect ~ Quantum Hall effect

  Hall Spin effect ~ Quantum Spin Hall effect

  Anomalous Hall Effect ~ Quantum AHE

（二）半导体材料的分类

按组成分：
- 无机半导体：元素、化合物
- 有机半导体

按结构分：
- 晶体：单晶体、多晶体
- 非晶、无定形

1.无机半导体晶体材料

无机半导体晶体材料包含元素半导体、化合物半导体及固溶体半导体。

(1)元素半导体晶体，如Si、Ge、Se 、C等

- In the 1920s, German scientists discovered that a “sandwich” of a selenium layer against another metal layer would pass current in only one direction.
- Se：0.08eV；类金属的能带结构；
- Si：间接带隙半导体（1.12eV），载流子迁移率较低，现代半导体工业的材料基础；优点：易氧化、高硬度，热稳定性好，便宜。
- Ge：锗有着良好的半导体性质，如电子迁移率、空穴迁移率等等。锗的发展仍具有很大的潜力。现代工业生产的锗，主要来自铜、铅、锌冶炼的副产品

碳家族材料

➢碳是一种非金属元素，IVA族，化学符号：C，原子序数：6，电子构型为[He]$2s^2 2p^2$。以多种形式广泛存在于大气和地壳之中，碳的一系列化合物——有机物更是生命的根本。

➢单质碳的物理和化学性质取决于晶体结构，物理性质各自不同。

➢常见同素异形体：石墨、金刚石、C60、碳纳米管、石墨烯、碳纤维，无定形碳等

Sp^3

5.5eV

绝缘体

折射率高；

热导率高；

硬度高；

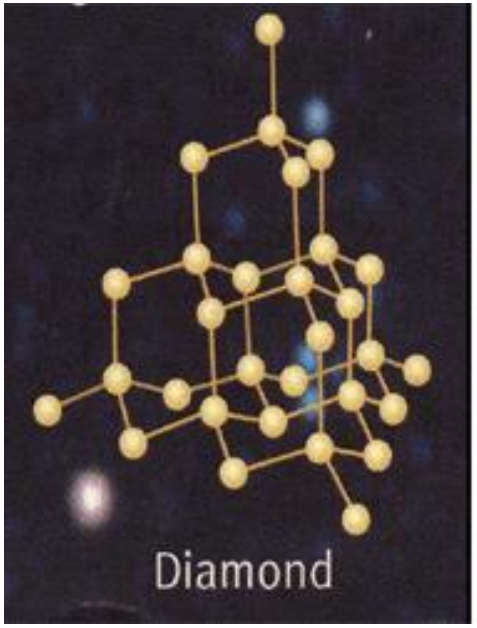

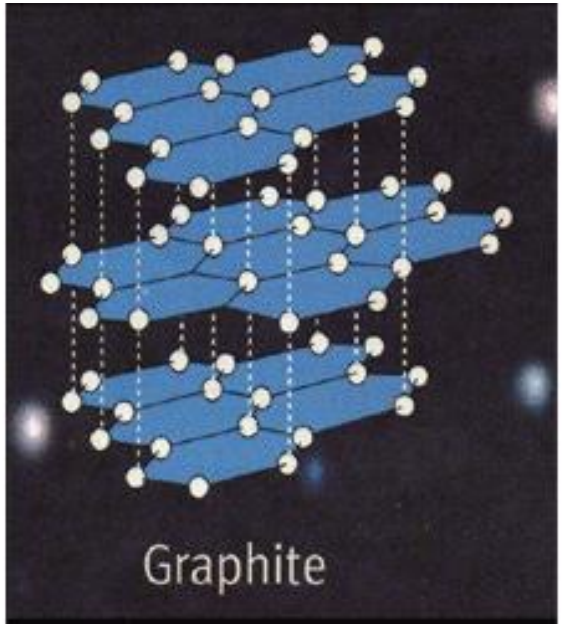

Sp^3

绝缘体

类自由电子

导热

导电

耐高温（3800）

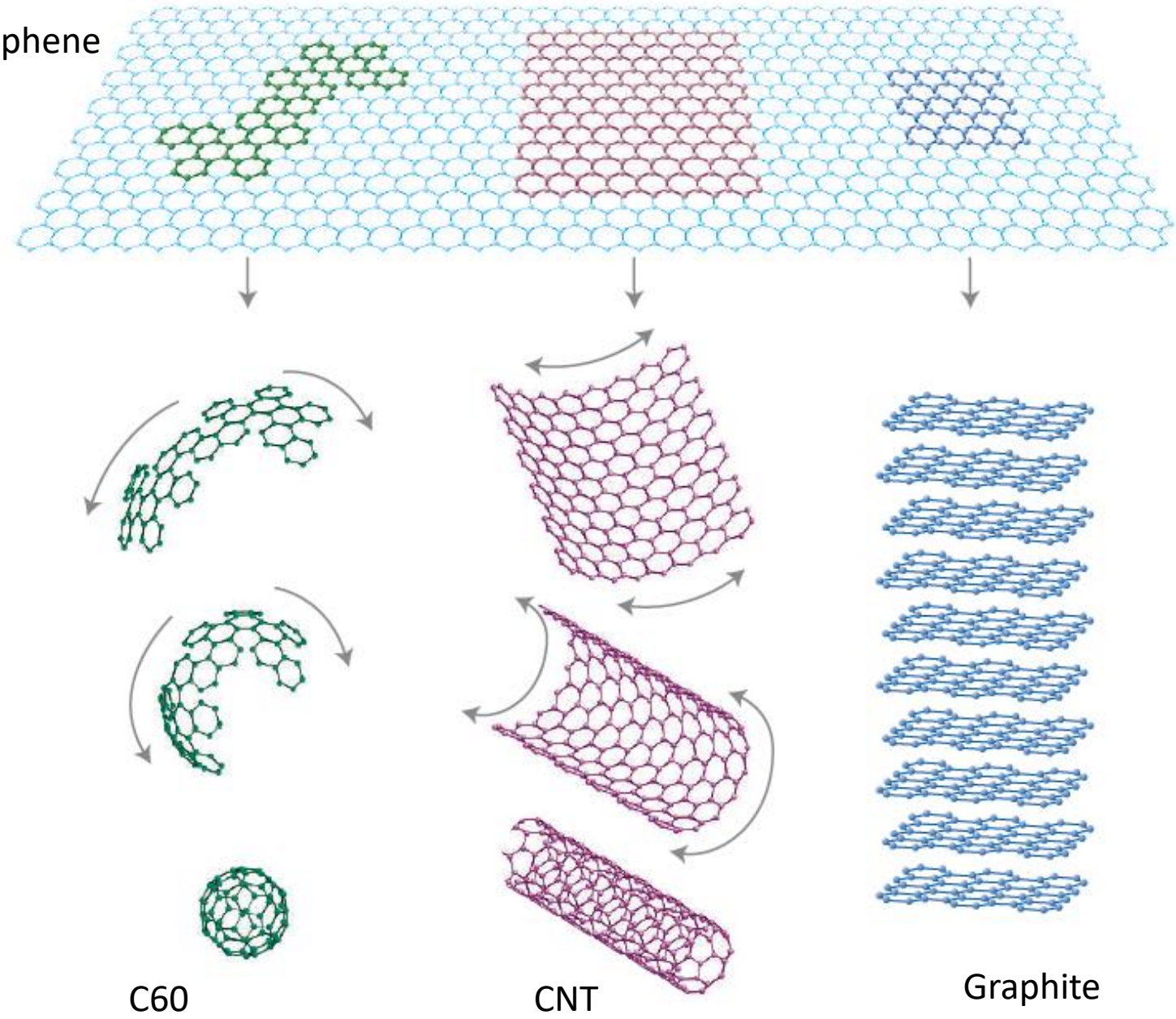

Figure 1 Mother of all graphitic forms. Graphene is a 2D building material for carbon materials of all other dimensionalities. It can be wrapped up into 0D buckyballs, rolled into 1D nanotubes or stacked into 3D graphite.

C60/Fullerene富勒烯/Buckyball巴基球

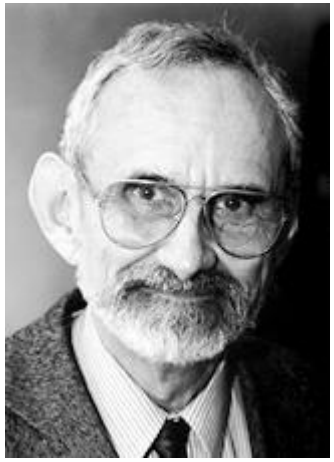
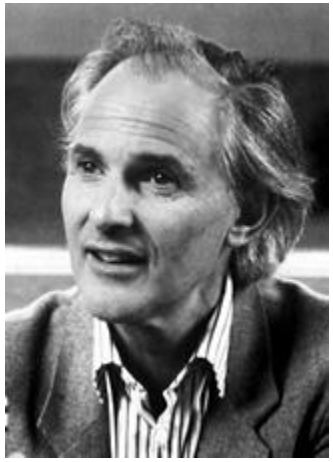
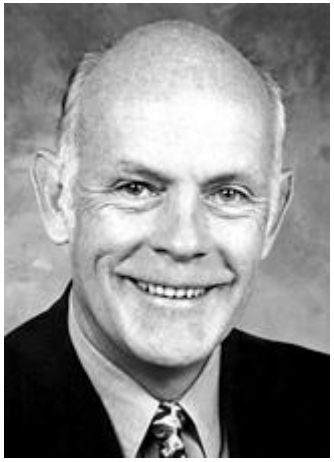
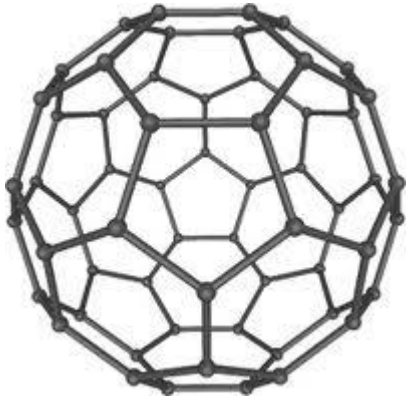

Robert F. Curl Jr.； Sir Harold W. Kroto； Richard E. Smalley;
"for their discovery of fullerenes"@ 1996 Nobel Prize in Chemistry

- 介于sp2与sp3之间；通过van de Waals形成固体.
- 直接带隙半导体，带隙1.7~2.3eV，较弱的室温荧光。
- 掺杂对C60的导电性影响很大，n/p掺杂
- Superconductivity

N-type OFET

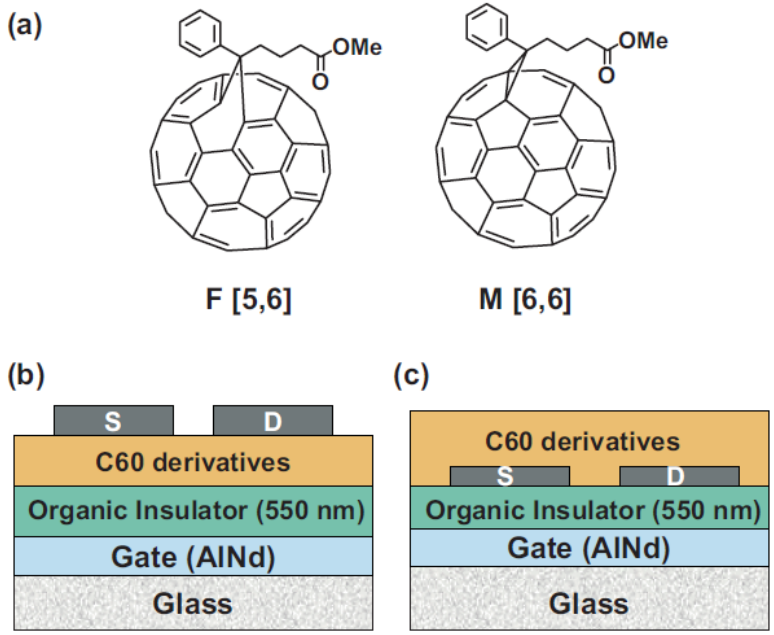

Figure 1. a) Chemical structures of the soluble fullerene derivatives used in the OTFTs. Fulleroid (1-(3-methoxycarbonyl)propyl-1-phenyl[5,6]C61) (F[5,6]) (left) and methanofullerene 1-(3-methoxycarbonyl)propyl-1-phenyl[6,6]C61 (M[6,6]) (right). b) The structure of a top-contact OTFT with a deposited AlNd gate on glass, a curable organic insulator (550 nm), soluble fullerene derivatives, and source–drain metal electrodes in sequence from bottom to top. c) The structure of a bottom-contact OTFT with a deposited AlNd gate on glass, a curable organic insulator (550 nm), source–drain metal electrodes, and soluble fullerene derivatives in sequence from bottom to top.

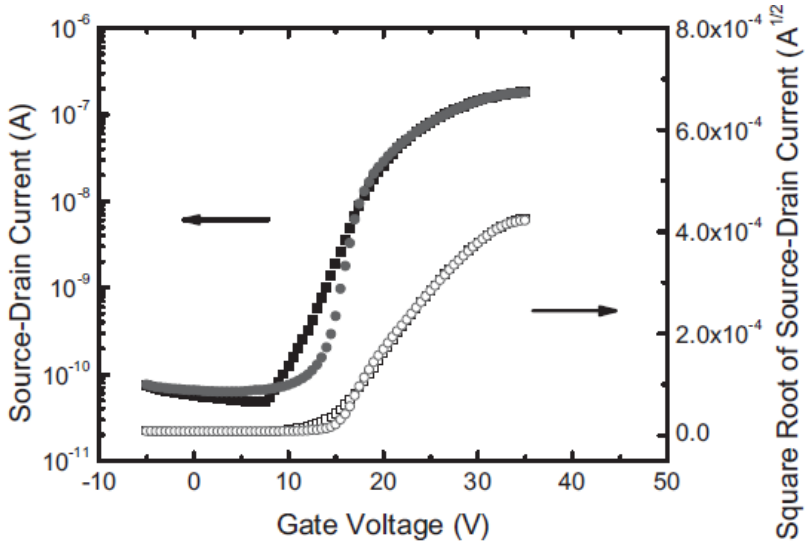

Workfunction of Source and Drain Metals (eV)

Figure 3. a) Transfer characteristics of the thin-film n-type transistors with Au electrodes based on F[5,6] (squares) and M[6,6] (circles). The devices are driven at a source–drain voltage (V_d) of 20 V. F[5,6] and M[6,6] were spin-cast at 1000 rpm spin speed. Both device mobilities were essentially the same (0.025 $cm^2 V^{-1} s^{-1}$). The transfer characteristics show that the threshold voltages of both the devices were also the same (13.6 V). b) Field-effect mobility versus the workfunction of source–drain

Adv. Mater. **2005**, *17*, 2180–2184

Graphene/石墨烯

The Nobel Prize in Physics 2010 was awarded jointly to Andre Geim and Konstantin Novoselov

"for groundbreaking experiments regarding the two-dimensional material graphene"

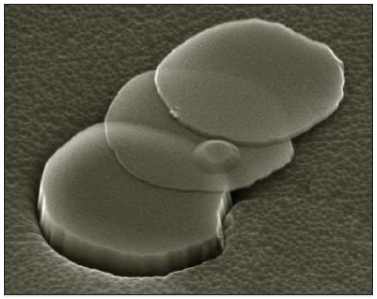

- It is the first truly two-dimensional crystalline materials and it is representative of a whole class of 2D materials.
- Density: 0.77mg/m^2
- Optical transparency: 2.3% in all optical domain
- Breaking strength: 42N/m
- Electrical conductivity: 200000 $cm^2S^{-1}V^{-1}$ @ $10^{12}cm^{-2}$; $R_{\square}$=31 ohm
- Thermal conductivity: 5000 $Wm^{-1}K^{-1}$

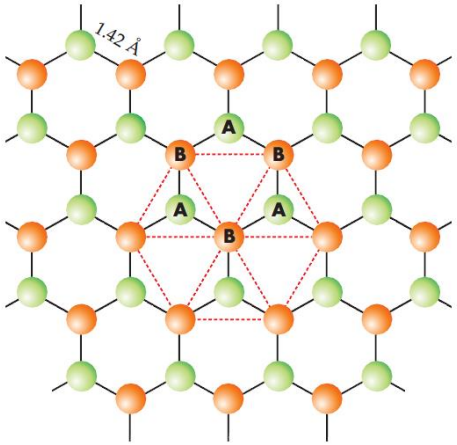

PRESSMEDDELANDE
Press release

5 October 2010

The Nobel Prize in Physics 2010

The Royal Swedish Academy of Sciences has decided to award the Nobel Prize in Physics for 2010 to

Andre Geim
University of Manchester, UK

and

Konstantin Novoselov
University of Manchester, UK

"for groundbreaking experiments regarding the two-dimensional material graphene"

Graphene – the perfect atomic lattice

A thin flake of ordinary carbon, just one atom thick, lies behind this year's Nobel Prize in Physics. Andre Geim and Konstantin Novoselov have shown that carbon in such a flat form has exceptional properties that originate from the remarkable world of quantum physics.

3. What is graphene?

Graphene is a single layer of carbon packed in a hexagonal (honeycomb) lattice, with a carbon-carbon distance of 0.142 nm. It is the first truly two-dimensional crystalline material and it is representative of a whole class of 2D materials including for example single layers of Boron-Nitride (BN) and Molybdenum-disulphide (MoS_2), which have both been produced after 2004.[8]

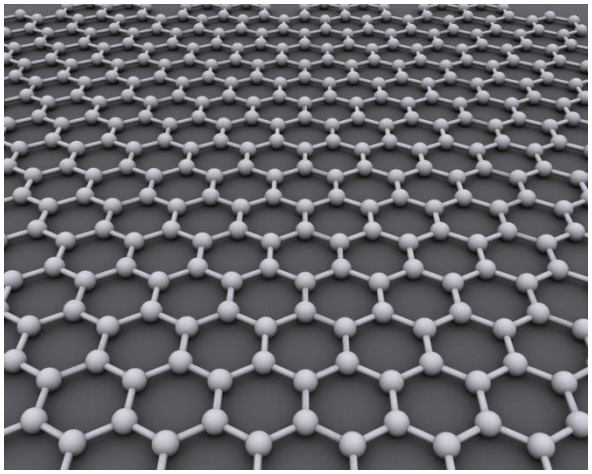

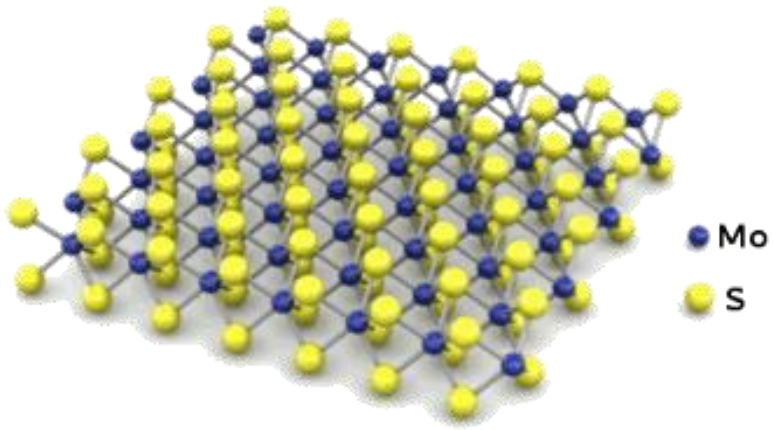

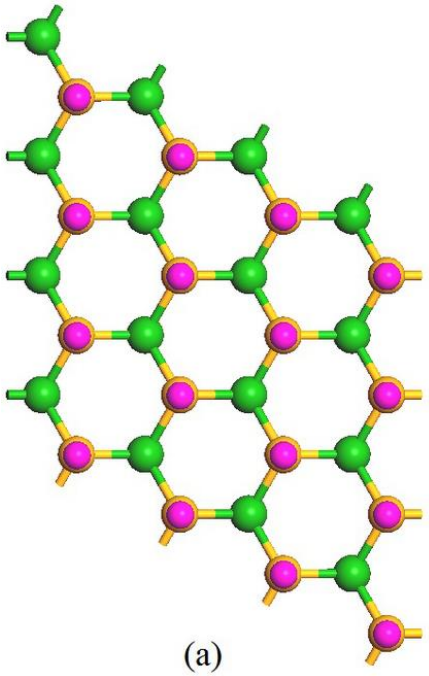

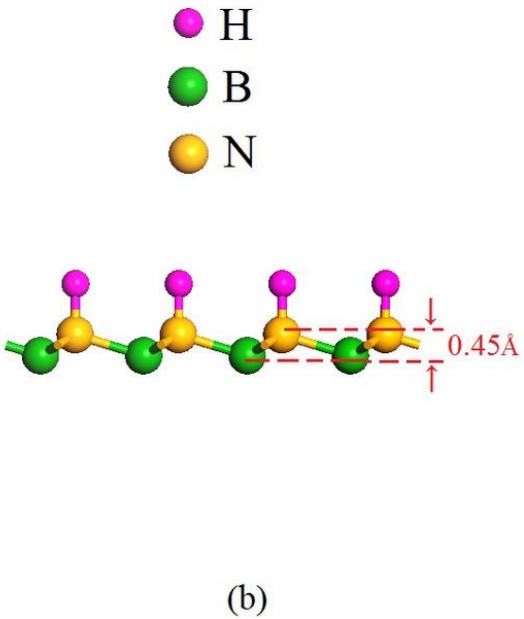

利用半导体物理语言对Graphene的基本描述

The electronic structure of graphene is rather different from usual three-dimensional materials. Its Fermi surface is characterized by six double cones, as shown in *Figure 2*. In intrinsic (undoped) graphene the Fermi level is situated at the connection points of these cones. Since the density of states of the material is zero at that point, the electrical conductivity of intrinsic graphene is quite low and is of the order of the conductance quantum $\sigma \sim e^2/h$; the exact prefactor is still debated. The Fermi level can however be changed by an electric field so that the material becomes either n-doped (with electrons) or p-doped (with holes) depending on the polarity of the applied field. Graphene can also be doped by adsorbing, for example, water or ammonia on its surface. The electrical conductivity for doped graphene is potentially quite high, at room temperature it may even be higher than that of copper.

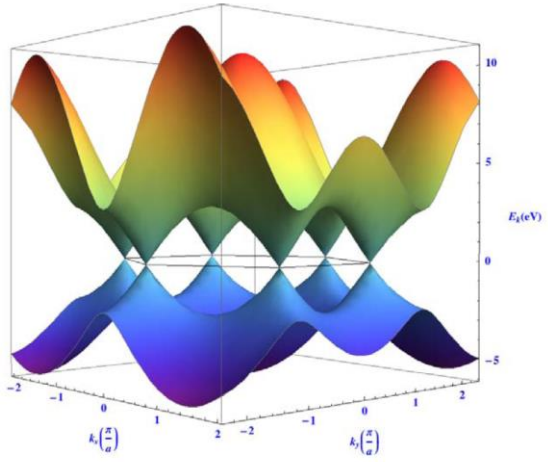

Figure 2. The energy, E, for the excitations in graphene as a function of the wave numbers, k_x and k_y, in the x and y directions. The black line represents the Fermi energy for an undoped graphene crystal. Close to this Fermi level the energy spectrum is characterized by six double cones where the dispersion relation (energy versus momentum, $\hbar k$) is linear. This corresponds to massless excitations.

Electron states in Graphene

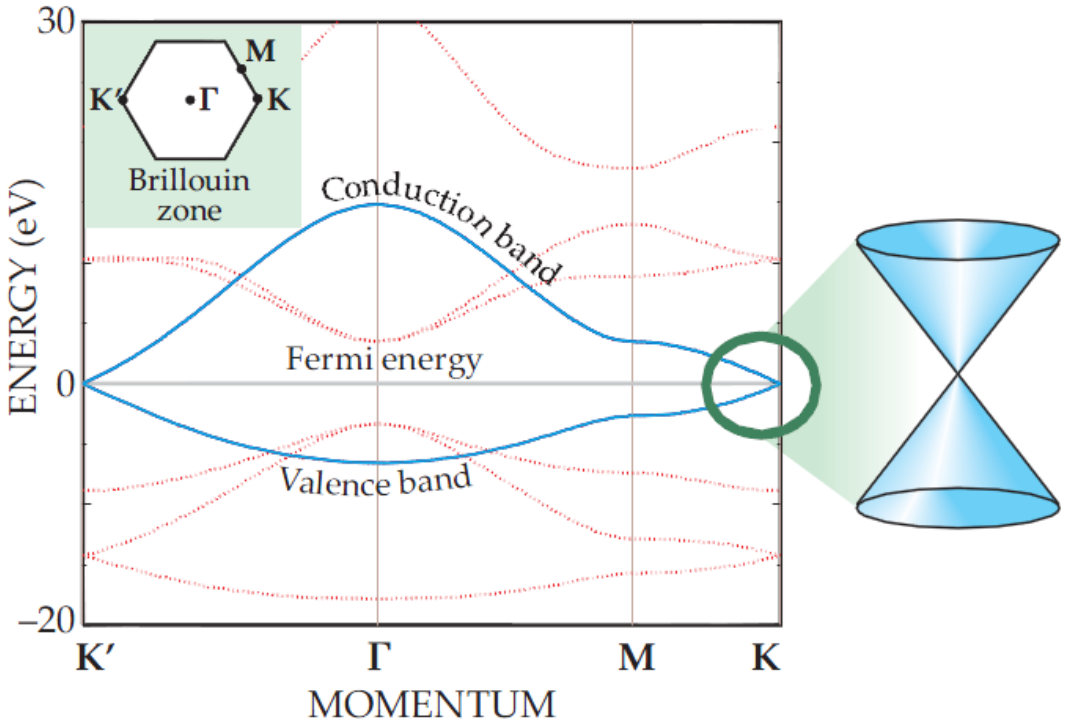

- 金属（零带隙半导体）
- n/p controlled by chemical doping or electrical
- 线性色散关系
- Massless Dirac Fermions in monolayer graphene exhibiting QHE

Density of graphene

The unit hexagonal cell of graphene contains two carbon atoms and has an area of 0.052 nm^2. We can thus calculate its density as being 0.77 mg/m^2. A hypothetical hammock measuring 1m^2 made from graphene would thus weigh 0.77 mg.

Optical transparency of graphene

Graphene is almost transparent, it absorbs only 2.3% of the light intensity, independent of the wavelength in the optical domain. This number is given by $\pi\,\alpha$, where α is the fine structure constant. Thus suspended graphene does not have any color.

Strength of graphene

Graphene has a breaking strength of 42N/m. Steel has a breaking strength in the range of 250-1200 MPa= 0.25-1.2x10^9 N/m^2. For a hypothetical steel film of the same thickness as graphene (which can be taken to be 3.35Å=3.35x10^{-10} m, *i.e.* the layer thickness in graphite), this would give a 2D breaking strength of 0.084-0.40 N/m. Thus graphene is more than 100 times stronger than the strongest steel.

In our 1 m^2 hammock tied between two trees you could place a weight of approximately 4 kg before it would break. It should thus be possible to make an almost invisible hammock out of graphene that could hold a cat without breaking. The hammock would weigh less than one mg, corresponding to the weight of one of the cat's whiskers.

Electrical conductivity of graphene

The sheet conductivity of a 2D material is given by $\sigma = en\mu$. The mobility is theoretically limited to μ=200,000 $cm^2V^{-1}s^{-1}$ by acoustic phonons at a carrier density of n=10^{12} cm^{-2}. The 2D sheet resistivity, also called the resistance per square, is then 31 Ω. Our fictional hammock measuring 1m^2 would thus have a resistance of 31 Ω.

Using the layer thickness we get a bulk conductivity of 0.96x10^6 $\Omega^{-1}cm^{-1}$ for graphene. This is somewhat higher than the conductivity of copper which is 0.60x10^6 $\Omega^{-1}cm^{-1}$.

Thermal conductivity

The thermal conductivity of graphene is dominated by phonons and has been measured to be approximately 5000 $Wm^{-1}K^{-1}$. Copper at room temperature has a thermal conductivity of 401 $Wm^{-1}K^{-1}$. Thus graphene conducts heat 10 times better than copper.

利用材料学的语言，对graphene性质的描述

(2)化合物半导体及固溶体半导体

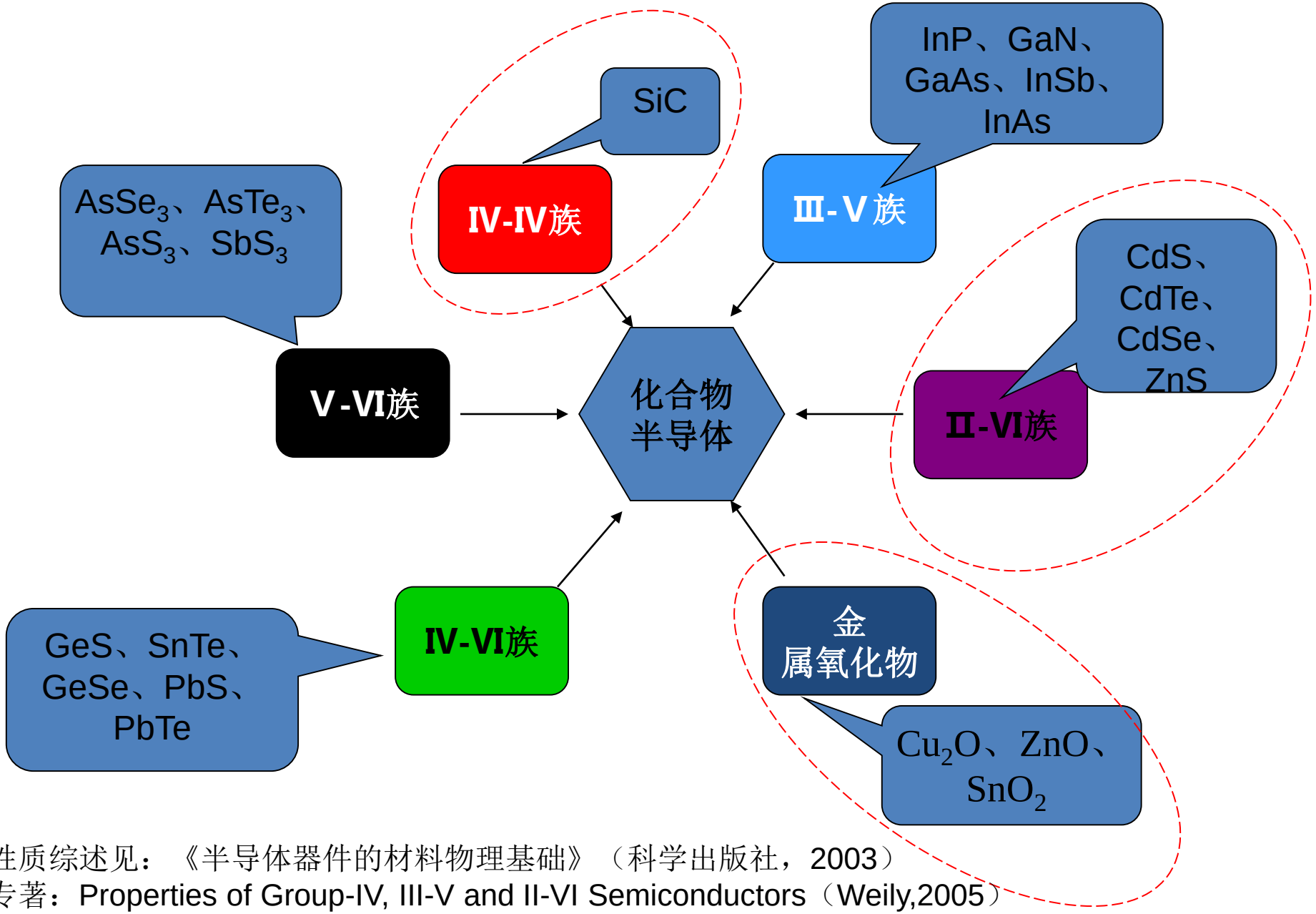

性质综述见：《半导体器件的材料物理基础》（科学出版社，2003）

专著：Properties of Group-IV, III-V and II-VI Semiconductors（Weily,2005）

II-IV 半导体的基本特点

- 研究历史比III-V早，但很不深入，有很多问题
- 高熔点，两种组份的蒸汽压不同，制备理想化学计量比的材料比较困难。
- 高密度空位等晶格缺陷，可以大范围影响其电导率
- 宽禁带，某些空位等缺陷的形成能较低，掺杂时容易发生自补偿效应，单极性材料
- CdTe除外，n/p均比较容易实现。
- 单极性材料器件往往只能采用MIS结构

氧化物半导体的基本特点

- 简单二元氧化物半导体：ZnO; CuO; Cu_2O; SnO; In_2O_3;
- 复杂的钙钛矿（perovskite）氧化物半导体：（BiTiO3….
- 作为陶瓷的半导体---铁电、压电、介电、多铁性能研究：grain / grain boundaries
- 单晶、外延薄膜、异质结等新材料体系
- 提高迁移率

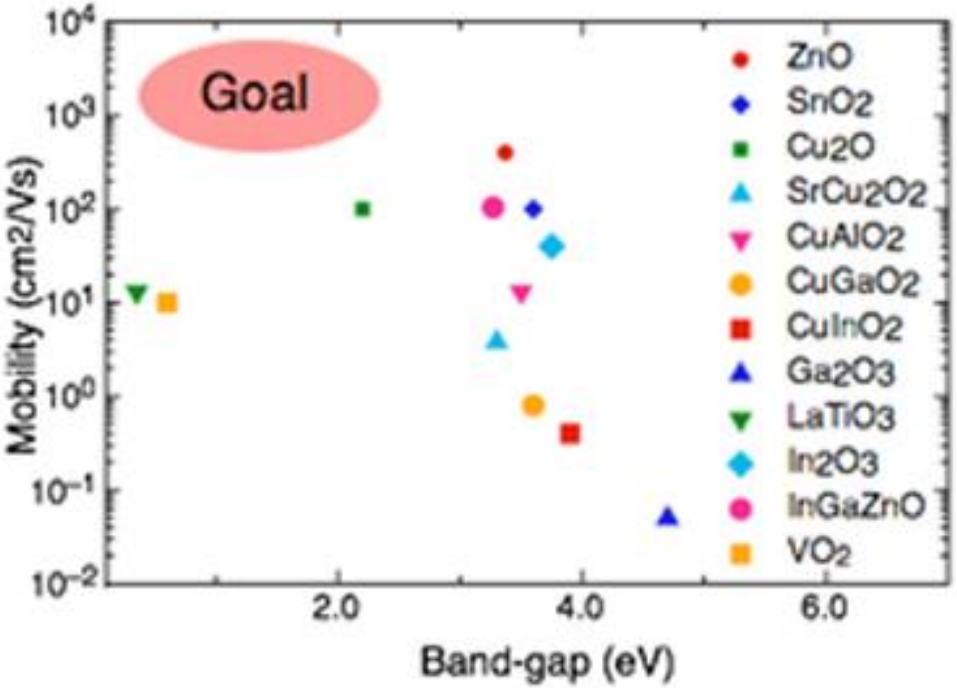

Figure 1 illustrates the reported carrier mobility versus the band gap for a whole range of oxide semiconductors.

TCO型半导体的典型应用领域

- **FPD technology**：as transparent conducting electrodes addressing each pixel, or larger zone, on the display screen; Flexible display

- **Aerospace:** Electromagnetic Shielding

- **Architectural glass :** Thermal Management (Low-emissivity glass); Electrochromic glass (Smart windows): Electrically induced reduction or bleaching of certain oxides (WO_3 and V_2O_5) results in an electrically controllable change in color and light transmission.

- **Solar energy**：TCO solar cell (SnO_2/Si@12%)；面电极（a-Si；CdS/CIS...）

- **Lighting** ：LED; OLED

- **Sensor**

- **TFT**

TCO型半导体发展历程

Year	Material (Ref.)	Year	Device (Ref.)
		1935	FET proposed [13]
1954	In_2O_3 TCO [1]	1954	Solar Cell [14]
1975	a-Si:H [11]		
		1979	a-Si:H TFT [12]
		1987	OLED [15]
1996	TAOS [5]		
1997	p-TCO, $CuAlO_2$ [2]		
		2000	All oxide pn-junction UV-LED [3]
2002	C12A7 transparent conductor [9]	2002	TOS homo-junction diode $CuInO_2$ [16]
		2004	TAOS-TFT [6]
2005	TiO_2:Nb TCO [8]	2005	ZnO homo-junction blue LED [17]
		2006	Front Drive Structure [18]
			ITO / organic gate TFT [19]
		2007	4.5" OLED using a-IGZO TFT [20]
		2008	12" OLED using a-IGZO TFT [7]
			15" LED using a-IGZO TFT [21]
			p-channel oxide TFT [22]

Figure 2.1 *Progress made in transparent oxide semiconductors and relevant devices*

Transparent Conductors

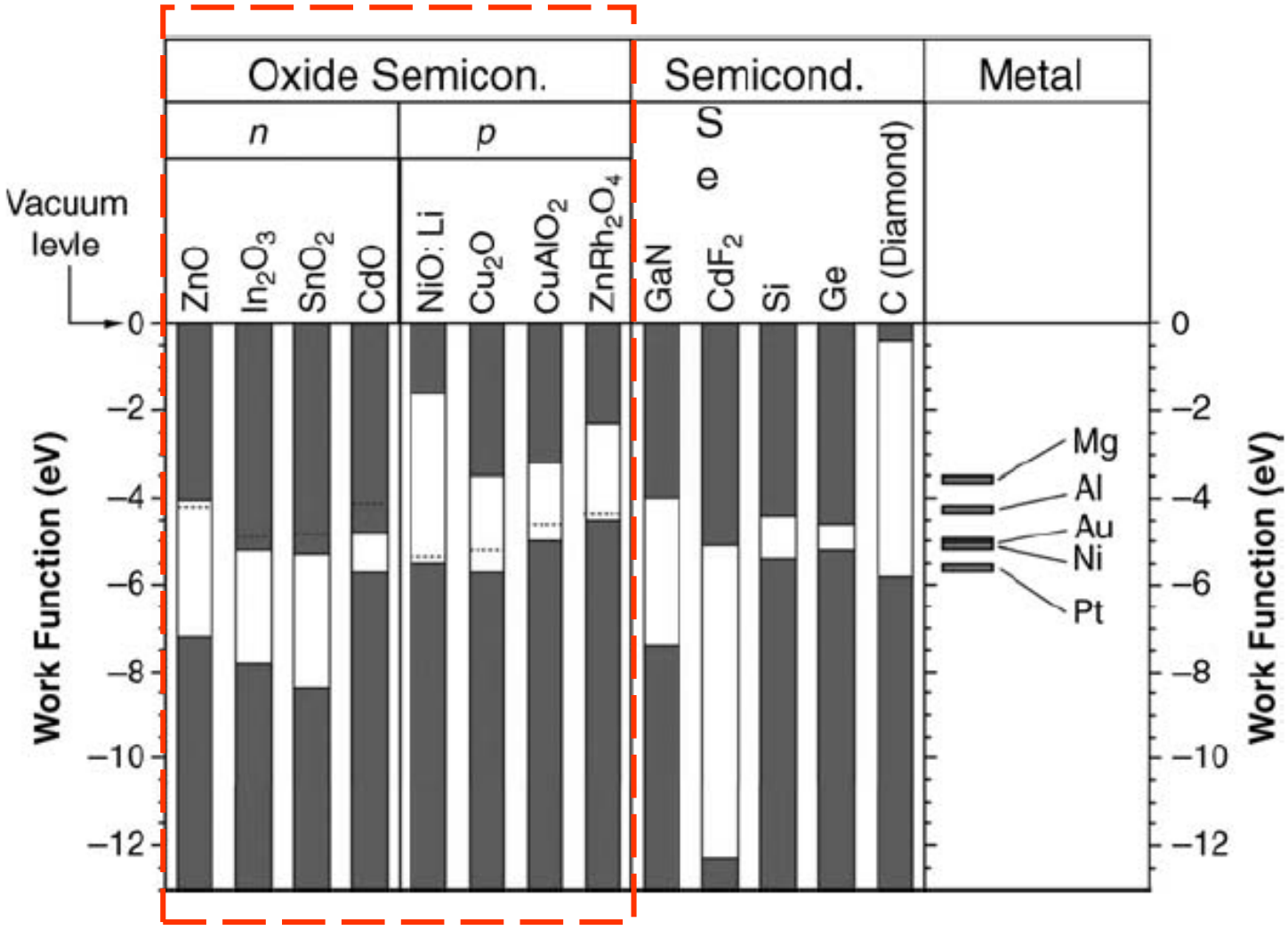

Figure 2.3 *Band line-up of oxide semiconductors and relevant materials*

Complex Perovskite Oxide Semiconductor

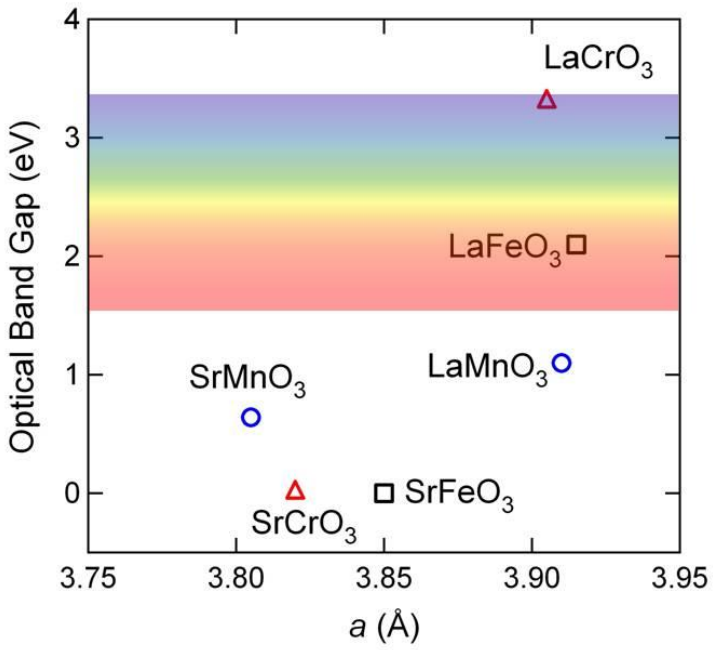

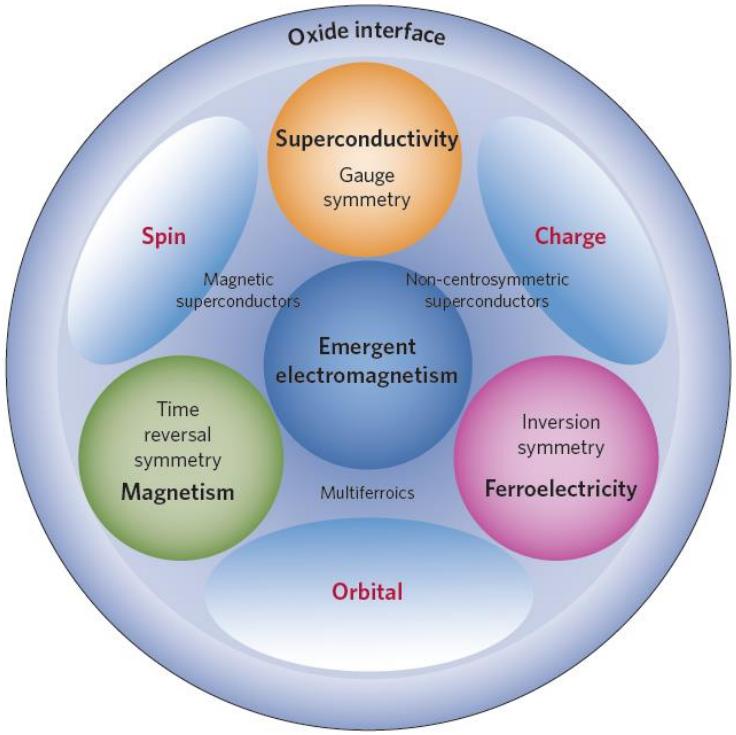

nature materials

REVIEW ARTICLE

PUBLISHED ONLINE: 24 JANUARY 2012 | DOI: 10.1038/NMAT3223

Emergent phenomena at oxide interfaces

H. Y. Hwang[1,2,3*], Y. Iwasa[1,3,4], M. Kawasaki[1,3,4], B. Keimer[5], N. Nagaosa[1,4] and Y. Tokura[1,4,6*]

Recent technical advances in the atomic-scale synthesis of oxide heterostructures have provided a fertile new ground for creating novel states at their interfaces. Different symmetry constraints can be used to design structures exhibiting phenomena not found in the bulk constituents. A characteristic feature is the reconstruction of the charge, spin and orbital states at interfaces on the nanometre scale. Examples such as interface superconductivity, magneto-electric coupling, and the quantum Hall effect in oxide heterostructures are representative of the scientific and technological opportunities in this rapidly emerging field.

另外几种典型的多元半导体

- 黄铜矿型三元半导体（$CuFeS_2$；$CdGeAs_2$；$AgGaS(e)_2$）：非线性光学，直接带隙；

- 太阳能电池用多元半导体：CIGS, $CH_3NH_3PbI_3$, $CsSnI_3$…

- 多元超导体：La_2CuO_4（2 eV）；La被Ba/Sr取代后，引入了足够多的空穴载流子，转变为超导体；e.g. $HgBaCa_2Cu_3O_{8+x}$（T_c=135K）

2.非晶态半导体

(1)非晶Si、非晶Ge以及非晶Te、Se元素半导体
(2)非晶化合物半导体有：GeTe、As_2Te_3、Se_4Te, ；IGZO film

3.有机半导体 (有机电子学)

（1）有机半导体通常分为有机分子晶体、有机分子络合物和高分子聚合物:PCBM; Spario, 。
（2）酞菁类及一些多环、稠环化合物，聚乙炔和环化脱聚丙烯腈等导电高分子，他们都具有大π键结构。

4.（稀）磁性半导体

（1）半导体本身就有磁性：NiO；FeO；CoO

（2）稀磁半导体（Diluted magnetic semiconductors, DMS）是指非磁性半导体中的部分原子被过渡金属元素（transition metals, TM）取代后形成的磁性半导体；因兼具有半导体和磁性的性质，即在一种材料中同时应用电子电荷和自旋两种自由度

三、常用半导体的生长技术

- 半导体材料的性质非常灵敏的依赖于其纯度和结构完整性；
- 生长：提纯和结构成型（不同维度、几何尺寸）
- 半导体晶体生长：获得高质量的大尺寸晶体
  - **高纯度、确定晶向、晶体结构完美的单晶体**
  - **用于切片，供半导体器件（外延）和集成电路**
- 半导体薄膜生长：获得高质量的薄膜
  - **高纯度、确定的orientation、厚度可控、界面可控**
  - **研究特殊物理效应的前提；器件的核心部分**
- 新型半导体器件：**材料的制备=器件的形成**

常用生长技术

晶体

- 直拉法（切克劳斯基法/Czochralski, CZ法）
- 区熔法（悬浮区熔法，Flouting Zone, FZ法）
- 布里奇曼法（Bridgman）
- …

薄膜/一维

- 溶胶-凝胶法
- 电化学沉积法
- 溅射法（Sputtering）：直流、交流溅射；磁控溅射，
- 化学/物理气相沉积（CVD/PVD/ALD）
- 激光脉冲沉积（PLD）
- 金属有机气相沉积（MOCVD）/氢化物气相外延（HVPE）
- 分子束外延（MBE）
- …

零维/一维

- 溶胶-凝胶
- 水热合成
- 激光烧蚀法
- …

半导体晶体生长技术概述

- 半导体晶锭通常是在特殊装置中通过熔体的定向缓慢冷却获得的；
  - 宏观上：熔体从一端开始沿固定方向一点一点逐渐凝固；
  - 微观上：所有凝固分子都受制于熔体前段的籽晶层引导，严格按籽晶的晶体取向排列起来。

- 获得大块、完美单晶

- 主要生长方法：
  - 直拉法、区熔法、布里奇曼法、….

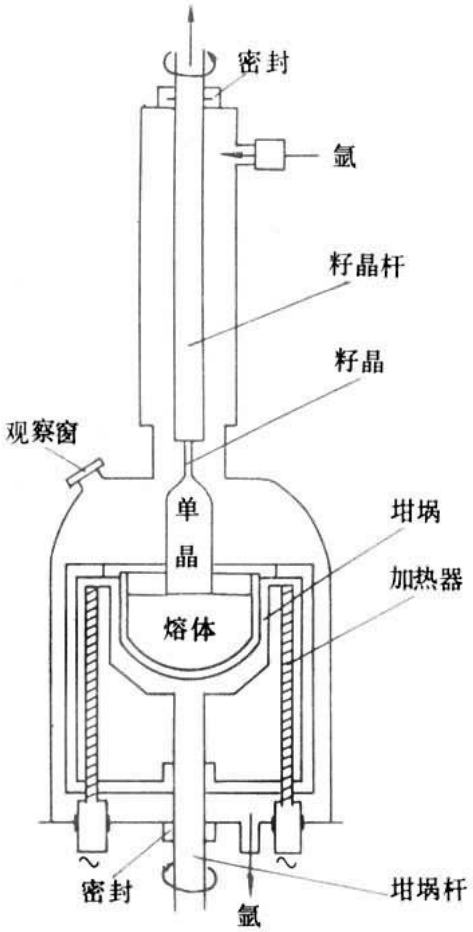

图1　直拉法晶体生长示意图

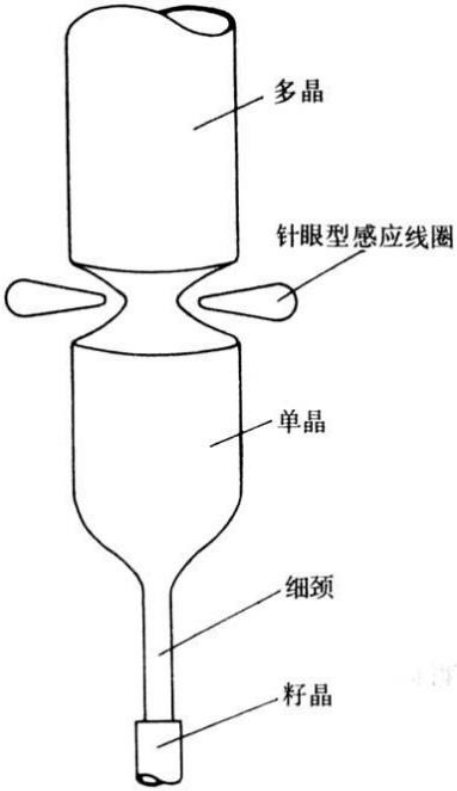

大直径硅单晶区熔生长法

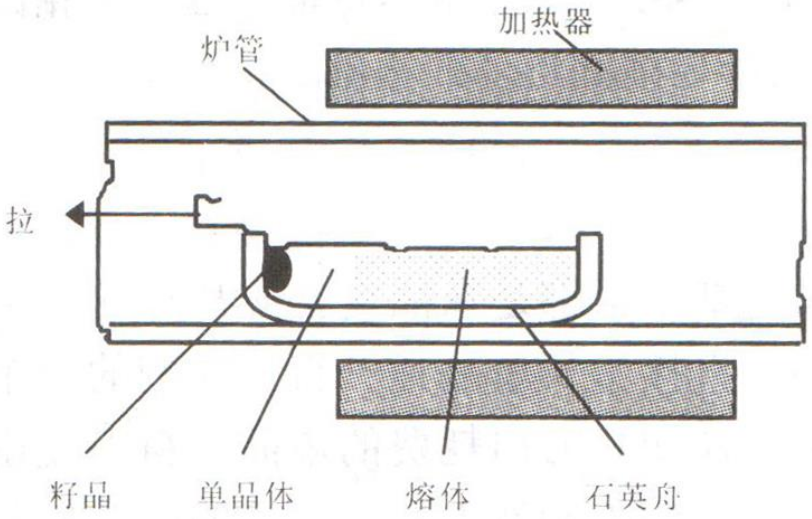

水平布里奇曼法实验装置示意图

（台湾SWI）

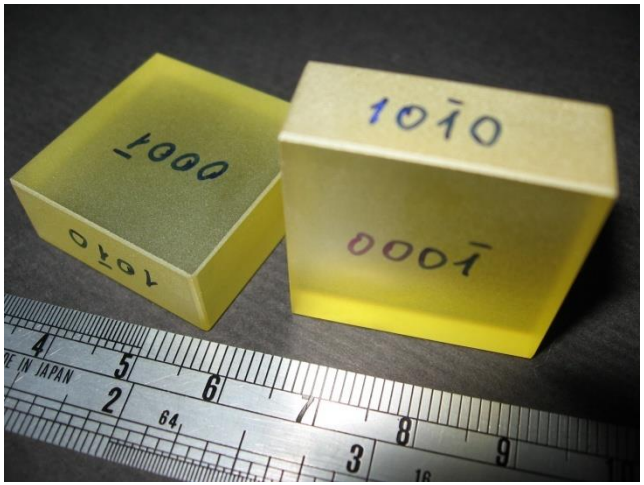

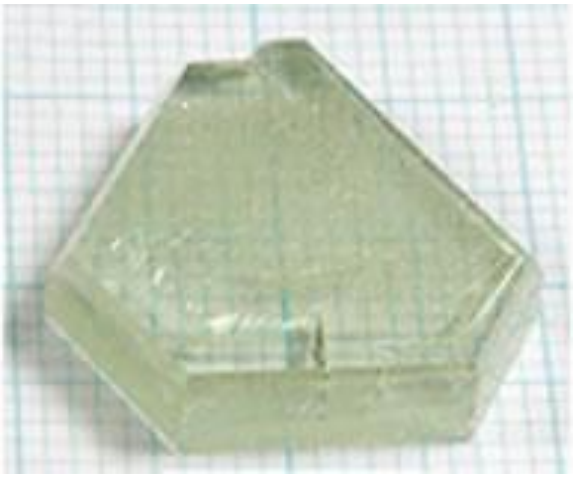

（日本东北大学）

北京工业大学

（国内大量小作坊）

半导体薄膜生长技术概述

• 薄膜生长的必要性

- 现在许多半导体器件只是用到芯片表面微米~纳米量级的一层薄膜；
- 这样的薄膜不可能通过切割大块晶体获得
- 单晶wafer只起衬底作用
- 半导体薄膜的制备已不是一种单纯的材料制备技术，而是器件制造工艺

•多晶/非晶薄膜沉积生长

- 对衬底要求不是很严格，生长窗口较宽

• 单晶薄膜外延生长

- 晶体外延：最重要的半导体薄膜生长方式

薄膜沉积

- **沉积：** The act of applying a thin film to a surface is *thin-film deposition* – any technique for depositing a thin film of material onto a substrate or onto previously deposited layers.

- **沉积生长的特点**
  - 衬底作为薄膜生长的载体，对其性质有一定影响，
  - 生长较快

- **沉积种类**
  - 化学沉积 (CBD/sol-gel, Spin-coating, ECD, CVD, …)
  - 物理沉积 (Thermal evaporation, Sputtering, PLD, ALD,…)

The steps of film deposition

1. Generation of a supply of atoms or molecules from a source, which may be solid, liquid, or vapor.

2. Transport of the constituent atoms or molecules to the substrate.
   - Uniform?

3. Deposition of atoms or molecules on the substrate.
   - Substrate effect?

4. Postgrowth treatment.
   - Annealing leading to crystal growth

5. Postgrowth analysis.

典型沉积方法 (一)

- CBD/sol-gel：
  - It uses a liquid precursor, usually a solution of organometallic powders dissolved in an organic solvent.
  - This is a relatively inexpensive, simple thin film process that is able to produce stoichiometrically accurate crystalline phases.
  - *Chemical Solution Deposition of Semiconductor Films*, Gary Hodes, Marcel Dekker, Inc, (2002)
  - (主要利用该制备方法的同学，查找相关文献资料，写一篇读书报告)

- Spin-coating:
  - It uses a liquid precursor, or sol-gel precursor deposited onto a smooth, flat substrate which is subsequently spun at a high velocity to centrifugally spread the solution over the substrate.
  - The speed at which the solution is spun and the viscosity of the sol determine the ultimate thickness of the deposited film.
  - Repeated depositions can be carried out to increase the thickness of films as desired.
  - Thermal treatment is often carried out in order to crystallize the amorphous spin coated film. Such crystalline films can exhibit certain preferred orientations after crystallization on single crystal substrates
  - (主要利用该制备方法的同学，查找相关文献资料，写一篇读书报告)

典型沉积方法（二）

- ECD：
  - Electrochemical Synthesis of Metal Oxides and Hydroxides, Chem. Mater. 2000, 12, 1195-1204.
  - Semiconductor Electrochemistry, Rüdiger Memming, Wiley, 2011
  - (主要利用该制备方法的同学，查找相关文献资料，写一篇读书报告)

- CVD：
  - Chemical vapor deposition (CVD) of thin films occurs when the reacting gas species come in contact with a heated substrate that catalyzes the reaction .
  - The substrate may supply the heat used to pyrolyze the reactant(s), or the entire reaction chamber may be heated.
  - Since CVD reactions are normally carried out at pressures in the range 0.5 to 10 Torr, gas-flow dynamics play a significant role in determining reaction rates and uniformity of the resulting films.
  - AP CVD, LP CVD, Plasma-enhanced CVD, MOCVD, Pulsed Laser assisted CVD, Hot wall CVD,…
  - (主要利用该制备方法的同学，查找相关文献资料，写一篇读书报告)

薄膜外延

- **外延**：在单晶衬底上，按照器件或电路设计所需要的电阻和厚度，沿衬底的结晶方向再生长一层新的单晶。
  - Layer-by-layer
  - 衬底部分的决定了外延薄膜的生长行为
- **外延生长的特点**
  - 掺杂浓度和薄膜厚度易于控制
  - 外延薄膜的物质属性、导电类型等易于控制，进而可形成异质结、pn结等
- **外延要求**
  - 低温（尽可能消除衬底因高温引起的影响：ZnO/saphire）
  - 厚度要精确控制
- **外延种类**
  - 气相外延、 液相外延、固相外延
  - Homoepitaxy、Heteroepitaxy

Importance of lattice mismatch

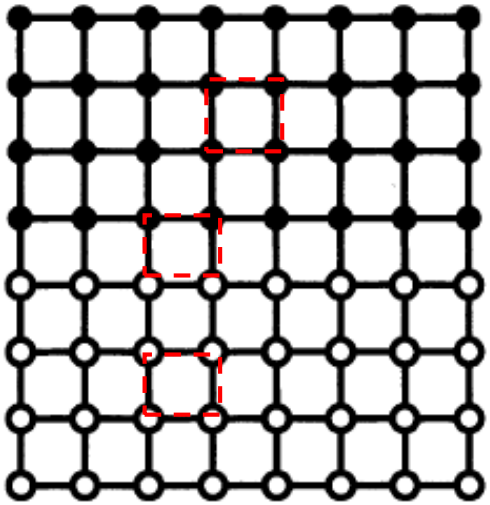

(a) commensurate growth with lattice matching,

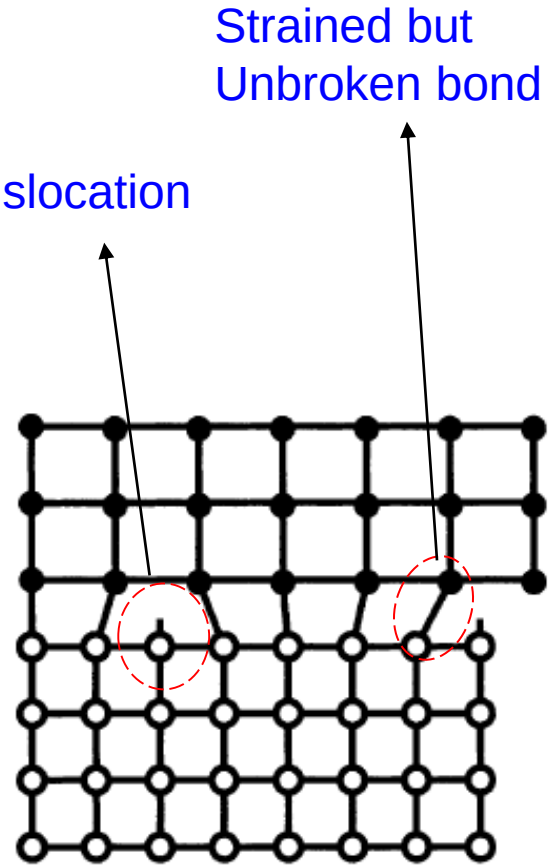

(b) strain-relaxed incommensurate growth

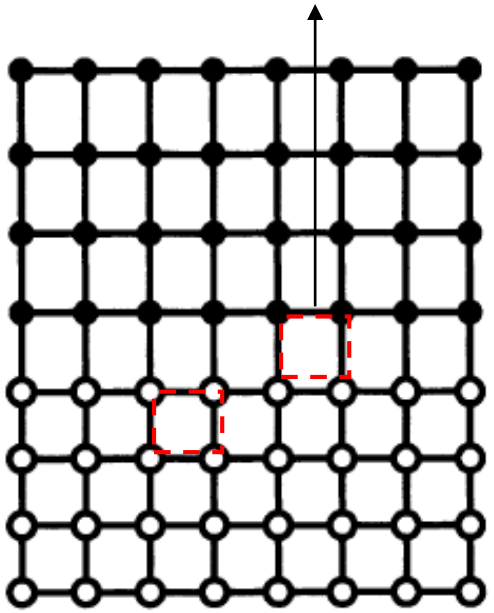

(c) pseudomorphic growth with uniaxial expansion normal to growth interface

液相外延

THIN FILMS

Spin coating epitaxial films

Meagan V. Kelso[1], Naveen K. Mahenderkar[1]*, Qingzhi Chen[2], John Z. Tubbesing[2], Jay A. Switzer[2]†

Spin-coated films, such as photoresists for lithography or perovskite films for solar cells, are either amorphous or polycrystalline. We show that epitaxial films of inorganic materials such as cesium lead bromide ($CsPbBr_3$), lead(II) iodide (PbI_2), zinc oxide (ZnO), and sodium chloride (NaCl) can be deposited onto a variety of single-crystal and single-crystal–like substrates by simply spin coating either solutions of the material or precursors to the material. The out-of-plane and in-plane orientations of the spin-coated films are determined by the substrate. The thin stagnant layer of supersaturated solution produced during spin coating promotes heterogeneous nucleation of the material onto the single-crystal substrate over homogeneous nucleation in the bulk solution, and ordered anion adlayers may lower the activation energy for nucleation on the surface. The method can be used to produce functional materials such as inorganic semiconductors or to deposit water-soluble materials such as NaCl that can serve as growth templates.

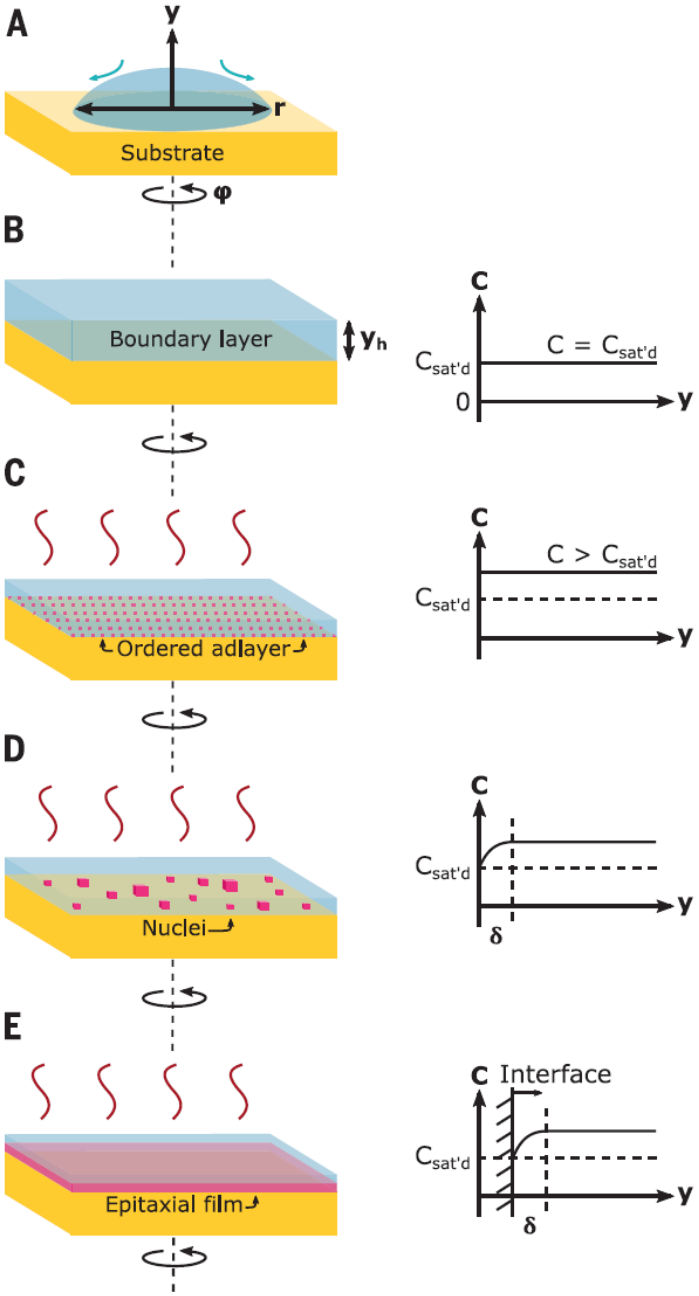
A
y
r
Substrate
φ
B
Boundary layer
y_h
C
$C_{sat'd}$
0
C = $C_{sat'd}$
y
C
C > $C_{sat'd}$
$C_{sat'd}$
y
C
Ordered adlayer
D
Nuclei
$C_{sat'd}$
δ
y
C
Interface
E
Epitaxial film
$C_{sat'd}$
δ
y

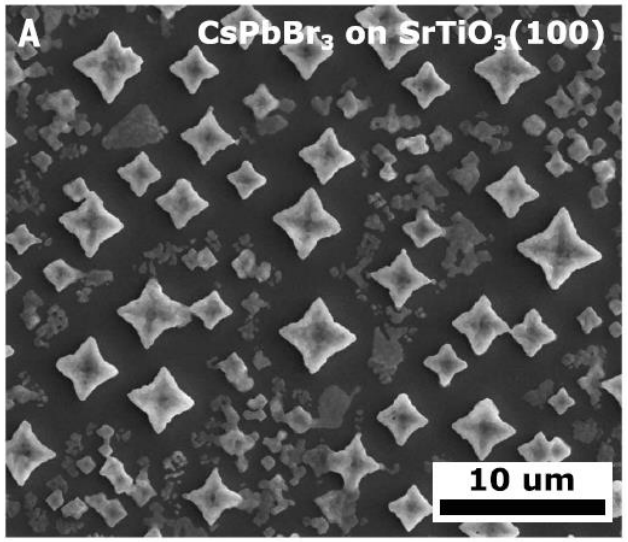
A
$CsPbBr_3$ on $SrTiO_3$(100)
10 um

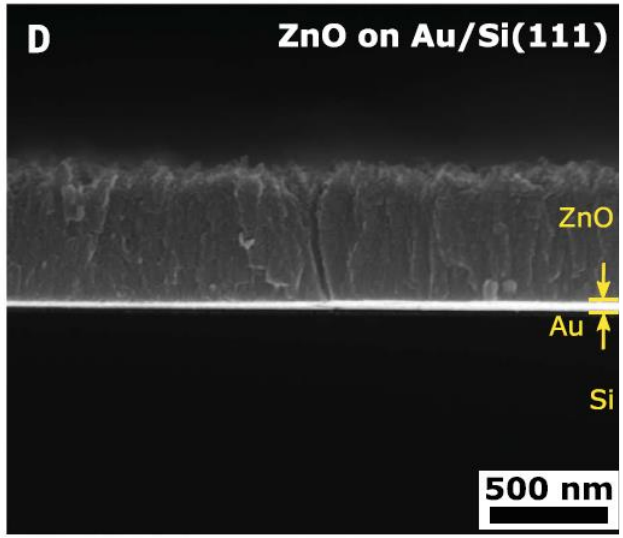
D
ZnO on Au/Si(111)
ZnO
Au
Si
500 nm

Science

TECHNICAL COMMENTS

Cite as: C. Lu, L. Tang, *Science* 10.1126/science.aay3894 (2019).

Comment on "Spin coating epitaxial films"

Chaojing Lu* and Lingli Tang

College of Physics, State Key Laboratory of Bio-Fibers and Eco-Textiles, Qingdao University, Qingdao, Shandong 266071, China.

***Corresponding author. Email: cjlu@qdu.edu.cn**

Kelso *et al.* (Reports, 12 April 2019, p. 166) claim that inorganic epitaxial films were deposited onto single-crystal or single-crystal–like substrates by spin coating. The epitaxial relationships were determined by x-ray diffraction. According to their pole figures, we estimate that each of their films contains only 4.1% to 25.5% epitaxial grains. None of their films can be considered epitaxial.

Science

TECHNICAL RESPONSES

Cite as: M. V. Kelso *et al.*, *Science* 10.1126/science.aay3966 (2019).

Response to Comment on "Spin coating epitaxial films"

Meagan V. Kelso,[1] Naveen K. Mahenderkar,[1]* Qingzhi Chen,[2] John Z. Tubbesing,[2] Jay A. Switzer[2]†

[1]Department of Materials Science and Engineering and Graduate Center for Materials Research, Missouri University of Science and Technology, Rolla, MO 65409, USA. [2]Department of Chemistry and Graduate Center for Materials Research, Missouri University of Science and Technology, Rolla, MO 65409, USA.

*Present address: Lam Research Corporation, 4650 Cushing Parkway, Fremont, CA 94538, USA.

†Corresponding author. Email: jswitzer@mst.edu

Lu and Tang claim that the spin-coated films in our study are not epitaxial. They assume that all of the background intensity in the x-ray pole figures of the spin-coated materials is due to randomly oriented grains. There is no evidence for randomly oriented grains in the 2θ x-ray patterns. The background intensity in the pole figures is also comparable to the background from the single-crystal substrates, which is inconsistent with their assumption.

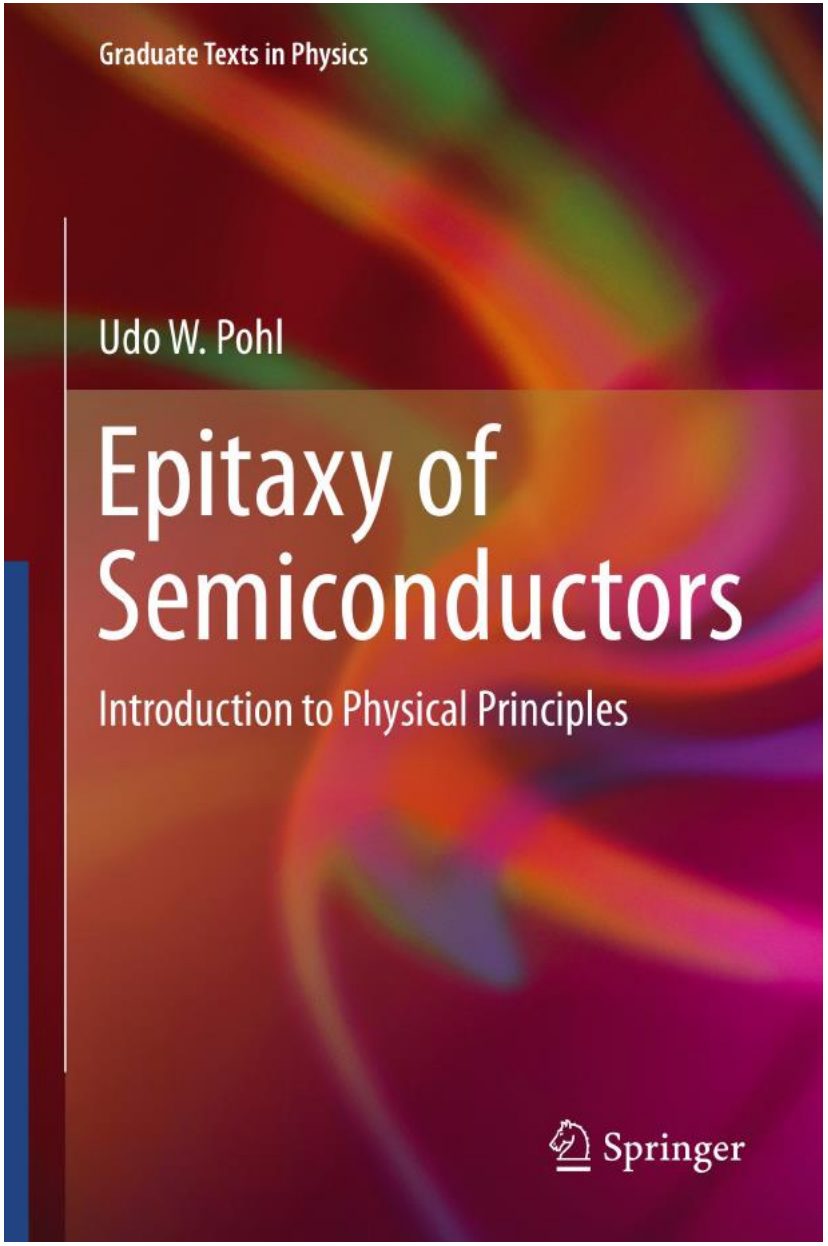

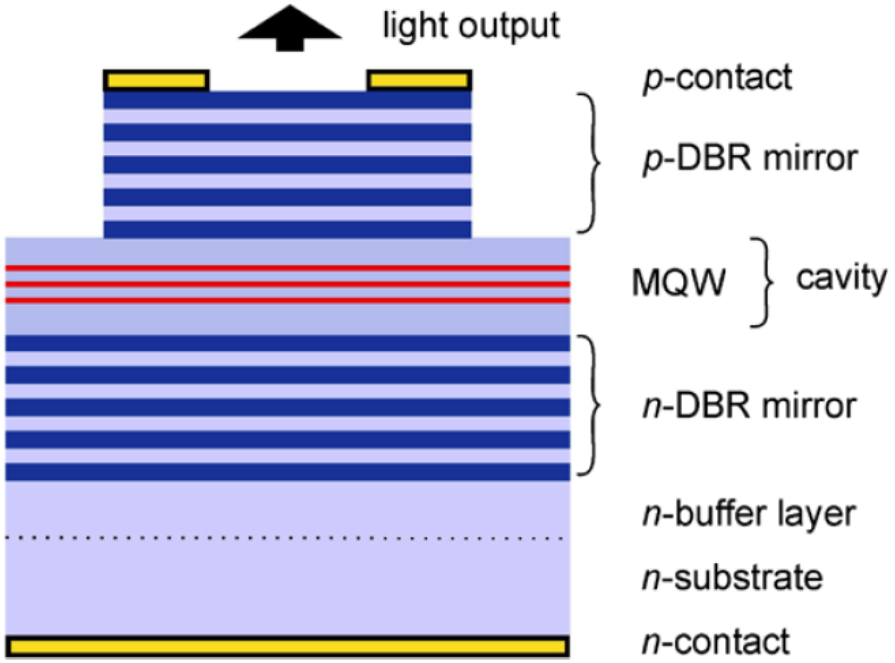

Fig. 1.3 Schematic of a vertical-cavity surface-emitting laser indicating the sequence of differently alloyed and doped semiconductor layers

MOCVD

Primarily used for II-VI, and III-V semiconductors, special metallic oxides and metals.

Metal Organic Chemical Vapor Deposition (MOCVD)

- Many materials that we wish to deposit have very low vapor pressures and thus are difficult to transport via gases.
- One solution is to chemically attach the metal (Ga, Al, Cu, etc…) to an organic compound that has a very high vapor pressure. Organic compounds often have very high vapor pressure (for example, alcohol has a strong odor).
- The organic-metal bond is very weak and can be broken via thermal means on wafer, depositing the metal with the high vapor pressure organic being pumped away.
- Care must be taken to insure little of the organic byproducts are incorporated. Carbon contamination and unintentional Hydrogen incorporation are sometimes a problem.

Human Hazard: As the human body absorbs organic compounds very easily, the metal organics are very easily absorbed by humans. Once in the body, the weak metal-organic bond is easily broken, thus, poisoning the body with heavy metals that often can not be easily removed by normal bodily functions. In extreme cases, blood transfusion is the only solution (if caught in time).

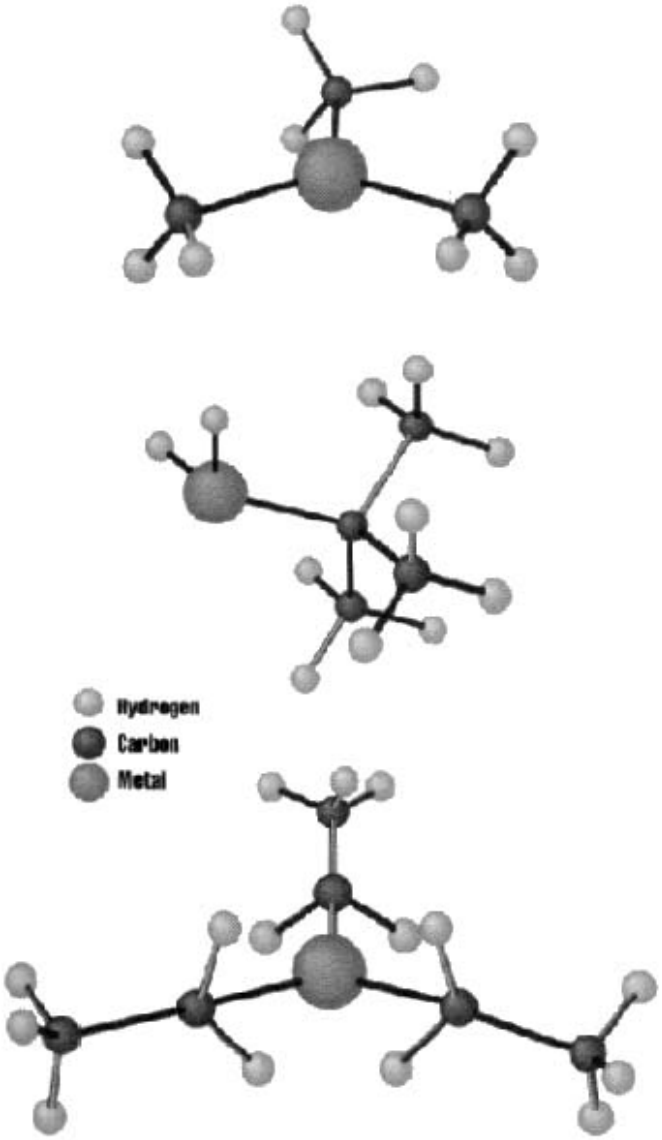

Figure 14-19 Examples of common organometallics used in MOCVD include (from top to bottom): trimethylgallium, tetrabutylarsine, and triethylgallium.

主要有德国爱思强(Aixtron，70%国际市场占有率)、

英国托马仕雯 (ThomasSwan，被Aixtron收购)、

美国维易科(Veeco，20%国际市场占有率)、美国Emcore(被Veeco收购)、

日本大阳酸素(Sanso，7%国际市场占有率,只在本国销售)

Commercial Thomas Swan® MOCVD

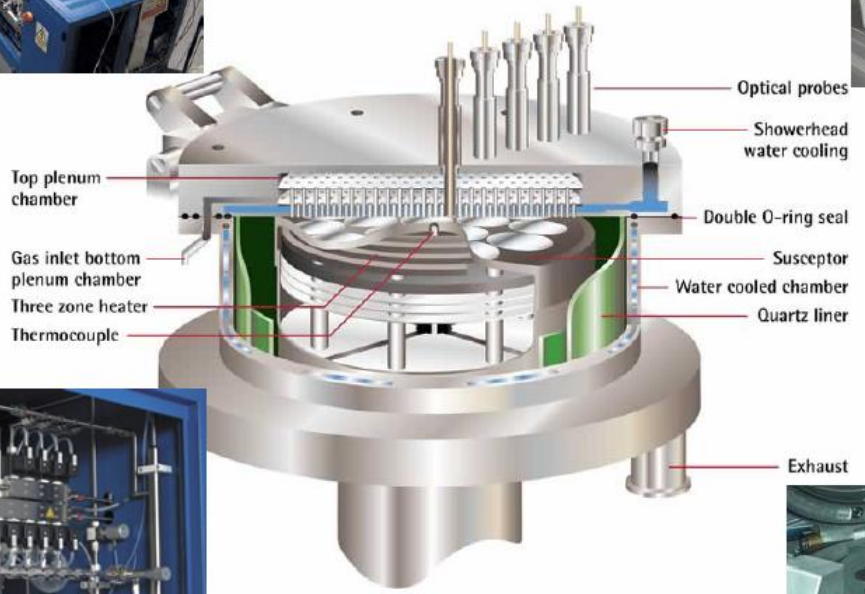

MBE

Dominates III-V electronic market and strong competitor in upper end LASER market
Offers the highest purity material (due to UHV conditions) and the best layer control (almost any fraction of an atomic layer can be deposited and layers can be sequenced one layer at a time (for example Ga then As then Ga etc…).

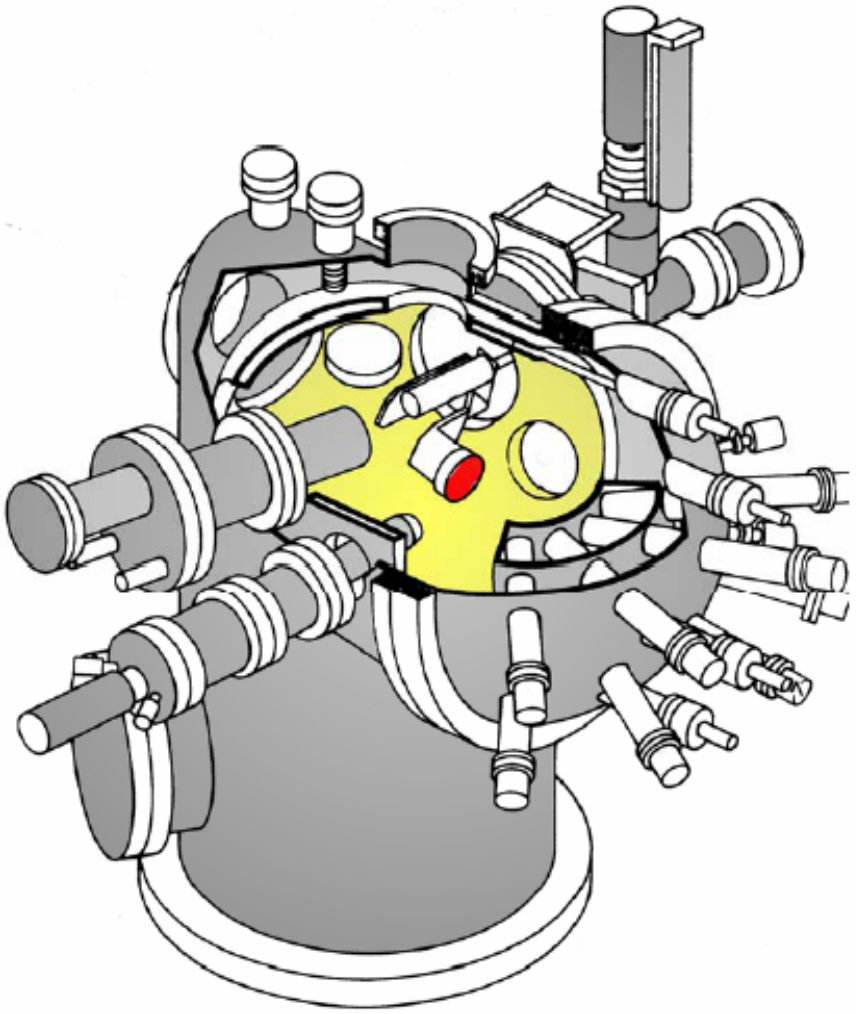

- In an UHV chamber, ultra high purity materials are evaporated.
- Because of the very low pressure, the mean free path is very long (can be hundreds of meters). Thus, the evaporated material travels in a straight line (a molecular beam) toward a hot substrate resulting in highly efficient raw materials usage.
- Once on the substrate, the atom or molecule moves around until it finds an atomic site to chemically bond to.
- Shutters can be used to turn the beam flux on and off
- The flux of atoms/molecules is controlled by the temperature of the "effusion cell" (evaporation source).

MBE

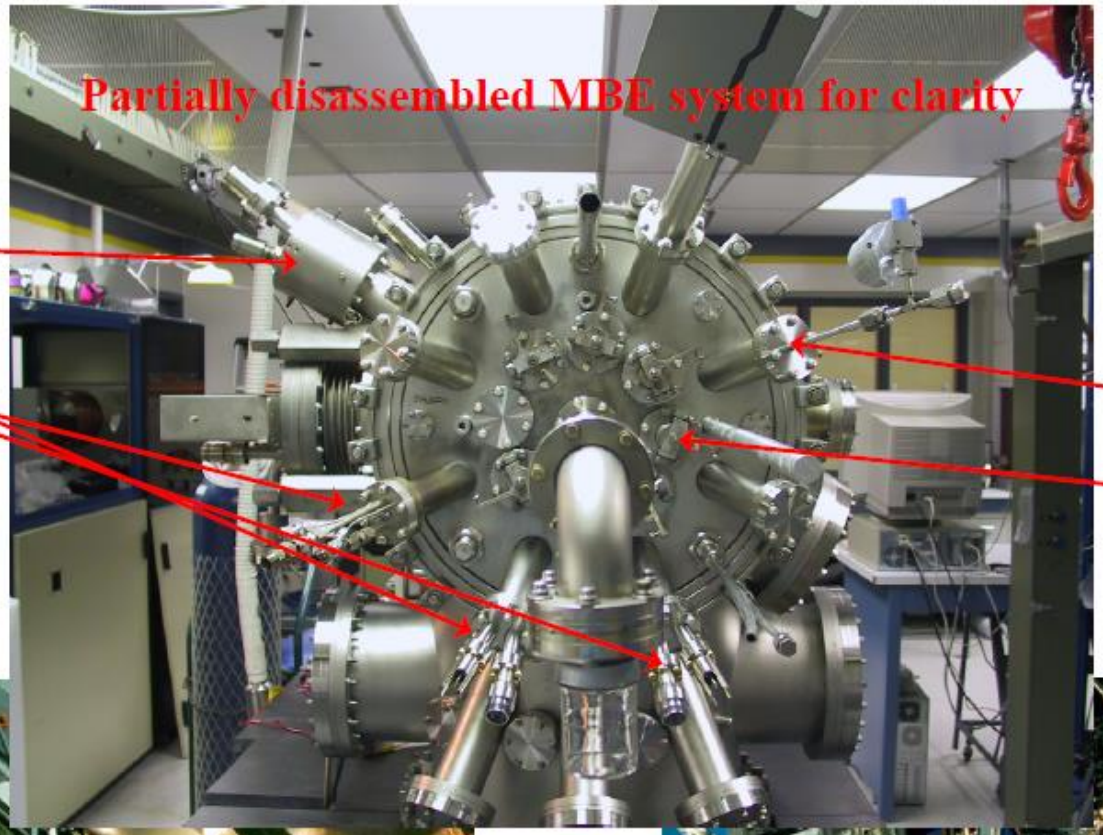
Partially disassembled MBE system for clarity
RHEED Gun
Effusion Furnaces

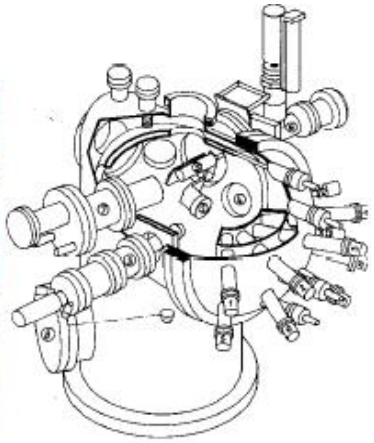
Gas Source (oxygen)
Shutter mechanism

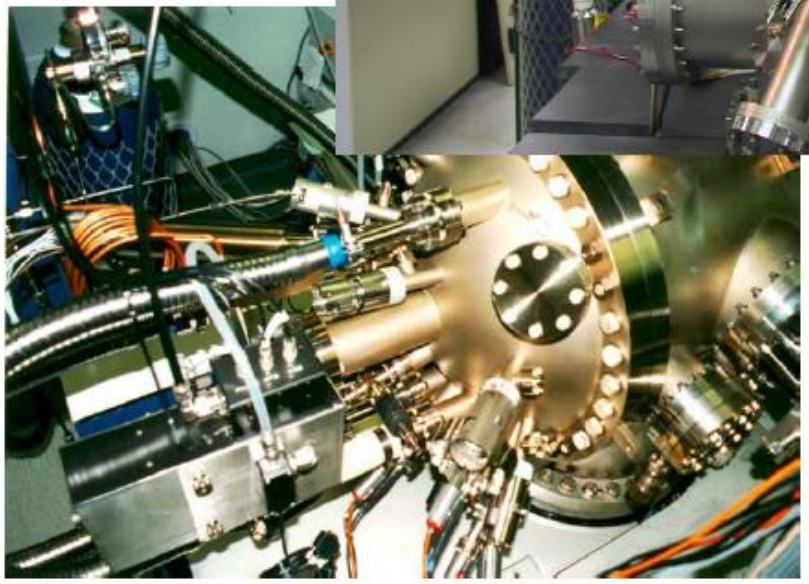

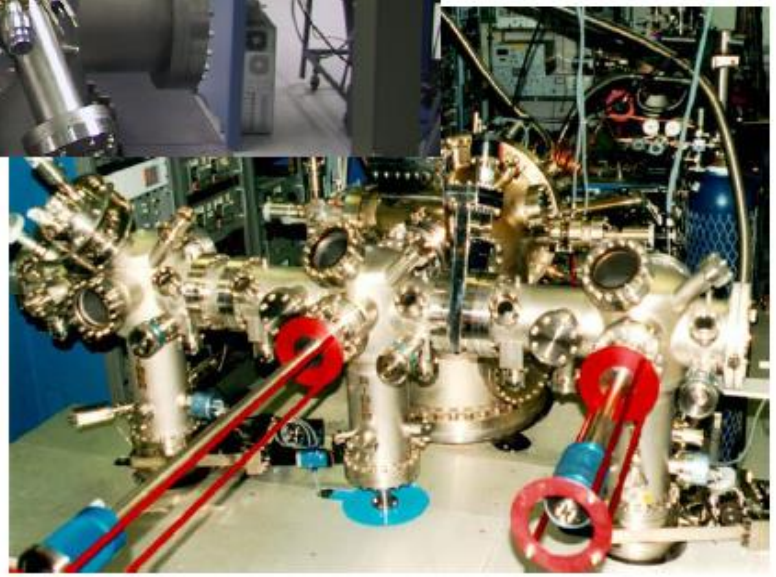

Pulsed Laser Deposition (PLD)

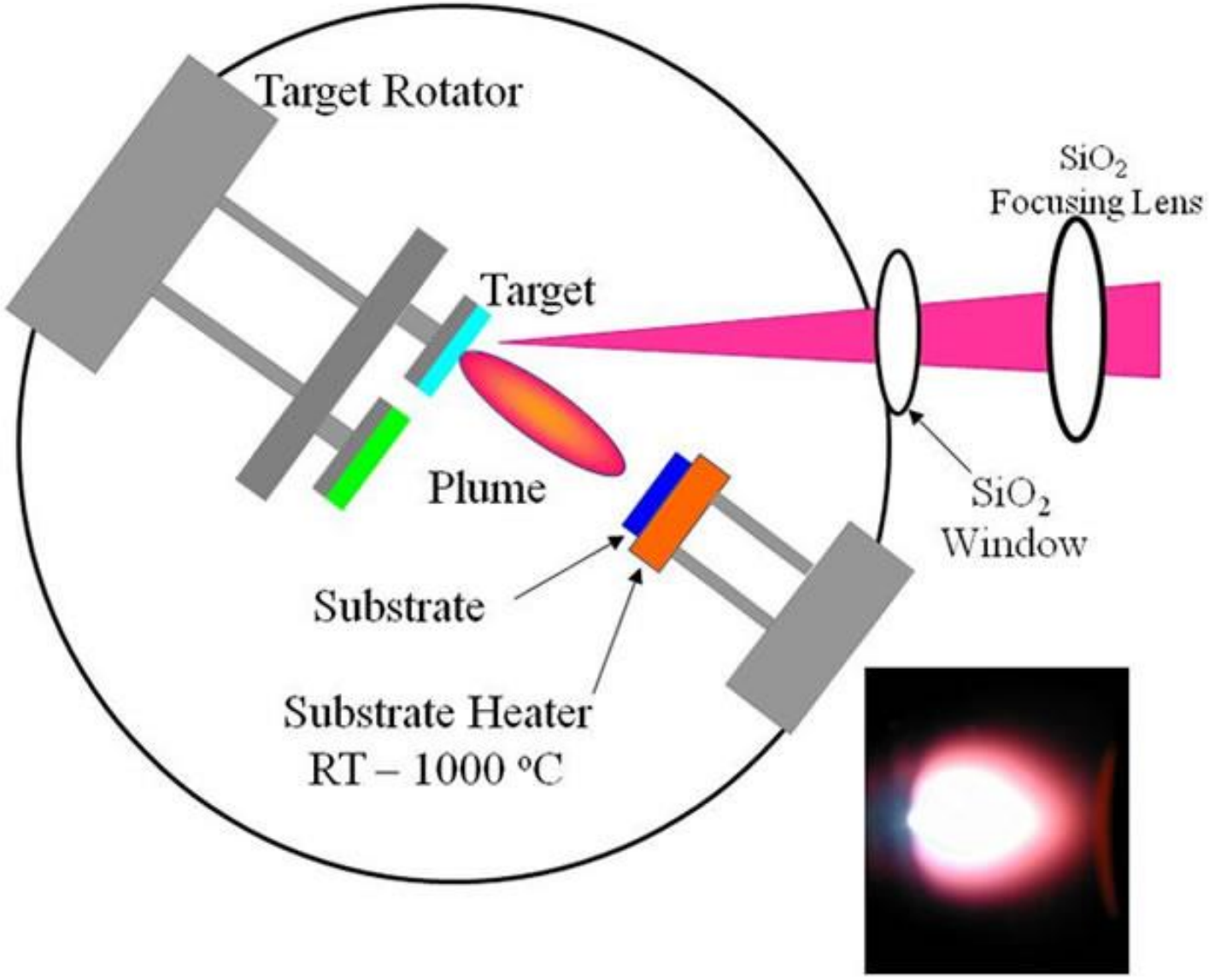


加热电源
KYKY

Pulsed Laser Deposition (readings)

- *Pulsed Laser Deposition of Thin Films*, edited by Douglas B. Chrisey and Graham K. Hubler, John Wiley & Sons, 1994

- *Pulsed Laser Deposition of Thin Films: Application-LED Growth of Functional Materials*, edited Robert Eason, John Wiley & Sons, 2007

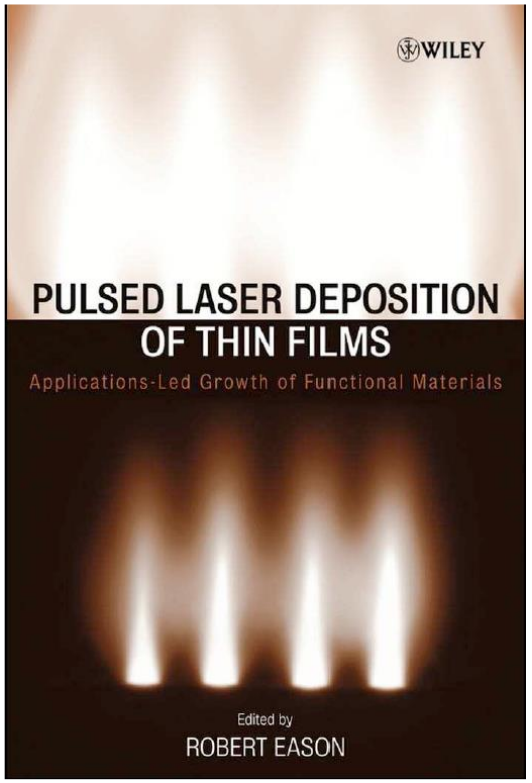

PLD + MBE = Laser MBE

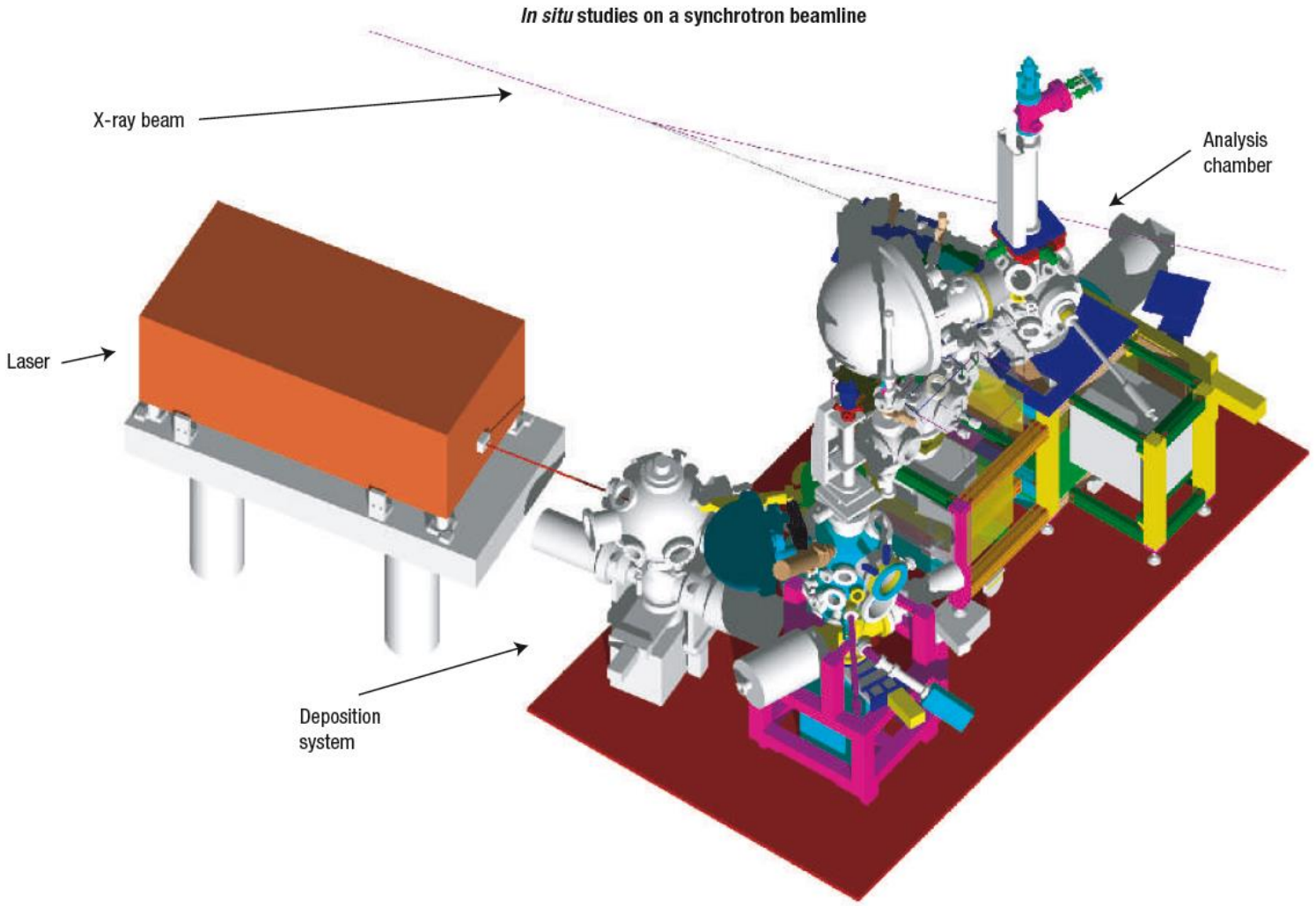

Figure 3 A schematic illustration of a thin-film deposition system (in this case a laser MBE system) that is attached to a synchrotron beamline. Such a system makes it easier to probe the electronic structure of surfaces and interfaces as the heterostructure is being grown. In the field of complex oxides, such *in situ* facilities are just emerging.

四、半导体的用途

Several Nobel Prizes have been awarded for discoveries and inventions in the field of semiconductor research.

1909
Karl Ferdinand Braun
(1850–1918)

1914
Max von Laue
(1879–1960)

1915
Sir William Henry Bragg
(1862–1942)

1915
William Laurence Bragg
(1890–1971)

1946
Percy Williams Bridgman
(1882–1961)

1953
William B. Shockley
(1910–1989)

1953
John Bardeen
(1908–1991)

1953
Walter Hauser Brattain
(1902–1987)

1973

Leo Esaki

(*1925)

1985

Klaus von Klitzing

(*1943)

1998

Robert B. Laughlin

(*1930)

1998

Horst L. Störmer

(*1949)

1998

Daniel C. Tsui

(*1939)

2000

Zhores I. Alferov

(*1938)

2000

Herbert Kroemer

(*1928)

2000

Jack St. Clair Kilby

(1923–2005)

2009

Willard S. Boyle

(1924–2011)

2009

George E. Smith

(*1930)

2010

Andre Geim

*1958

2010

Konstantin Novoselov

*1974

2014

Isamu Akasaki

(*1929)

2014

Hiroshi Amano

(*1960)

2014

Shuji Nakamura

(*1954)

2019 /10/08 (17:45)： Phys.

本章结语

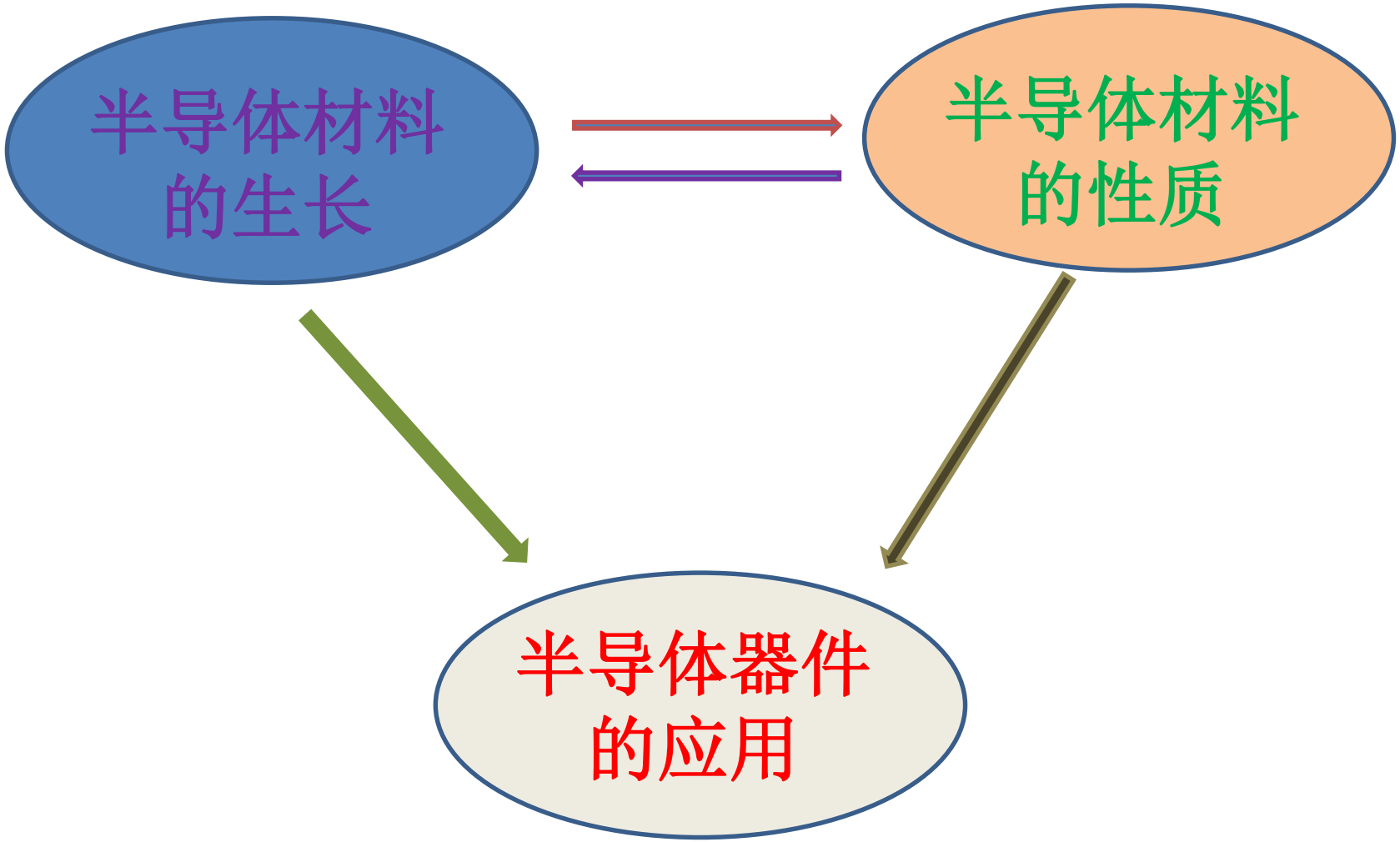

Table 1.3. Lattice constant a, energy gap E_G at 300 K, type of energy gap, and lattice structure of group IV elements.

Material	a (nm)	E_G (eV)	E_G (nm)	Type	Structure
Diamond (C)	0.357	5.48	226	indirect	cubic
Silicon (Si)	0.543	1.12	1107	indirect	cubic
Germanium (Ge)	0.566	0.664	1867	indirect	cubic
Gray tin (α-Sn)	0.649	—	—	—	cubic
White tin (β-Sn)	0.583 0.318	—	—	—	tetragonal
Graphite (C)	0.246 0.673	—	—	—	hexagonal
Lead (Pb)	0.495	—	—	—	cubic

Table 1.4. Lattice constant a, energy gap E_G at 300 K, type of energy gap, and lattice structure of III-V semiconductors.

Material	a (nm)	E_G (eV)	E_G (nm)	Type	Structure
BN	0.362	6.4	194	indirect	cubic
	0.666, 0.250	5.2	238	direct	hexagonal
AlN	0.311, 0.498	6.2	200	direct	hexagonal
GaN	0.318, 0.517	3.44	360	direct	hexagonal
AlP	0.546	2.51	494	indirect	cubic
BP	0.454	2.4	517	indirect	cubic
GaP	0.545	2.27	546	indirect	cubic
AlAs	0.566	2.15	577	indirect	cubic
InN	0.354, 0.870	1.89	656	direct	hexagonal
AlSb	0.614	1.62	765	indirect	cubic
GaAs	0.565	1.424	871	direct	cubic
InP	0.587	1.34	925	direct	cubic
GaSb	0.610	0.75	1653	direct	cubic
InAs	0.606	0.354	3502	direct	cubic
InSb	0.648	0.18	6890	direct	cubic

Table 1.6. Lattice constant a, energy gap E_G at low temperature, type of energy gap, and lattice structure of I-VII semiconductors.

Material	a (nm)	E_G (eV)	E_G (nm)	Type	Structure
γ-CuCl	0.541	3.395	365	direct	cubic
AgCl	0.555	3.249	382	indirect	cubic
γ-CuI	0.604	3.115	398	direct	cubic
γ-CuBr	0.569	3.077	403	direct	cubic
β-AgI	0.458, 0.749	3.024	410	direct	hexagonal
AgBr	0.577	2.684	462	indirect	cubic

Table 1.5. Lattice constant a, energy gap E_G at 300 K (* denotes value at low temperature), type of energy gap, and lattice structure of II-VI semiconductors.

Material	a (nm)	E_G (eV)	E_G (nm)	Type	Structure
ZnS	0.541	3.68	337	direct	cubic
	0.382, 0.626	3.91	317	direct	hexagonal
ZnO	0.325, 0.521	3.44*	360	direct	hexagonal
ZnSe	0.567	2.7	459	direct	cubic
	0.40, 0.654			direct	hexagonal
CdS	0.582	2.55	486	direct	cubic
	0.414, 0.671	2.51	494	direct	hexagonal
ZnTe	0.610	2.28	544	direct	cubic
α-HgS	0.415, 0.950	2.1	590	direct	trigonal
β-HgS	0.585	—	—	—	cubic
CdSe	0.605	1.9*	653	direct	cubic
	0.43, 0.701	1.75	709	direct	hexagonal
CdTe	0.648	1.475	841	direct	cubic
HgSe	0.609	—	—	—	cubic
HgTe	0.646	—	—	—	cubic

重要半导体参数汇总

	E_g (eV)	μ_n (cm^2/V-s)	μ_p (cm^2/V-s)	Transition	Lattice	a (Å)	ϵ_r	Density (g/cm^3)	Melting point (°C)
Si	1.11	1350	480	*i*	*D*	5.43	11.8	2.33	1415
Ge	0.67	3900	1900	*i*	*D*	5.65	16	5.32	936
SiC(α)	2.86	500		*i*	*W*	3.08	10.2	3.21	2830
AlP	2.45	80		*i*	*Z*	5.46	9.8	2.40	2000
AlAs	2.16	180		*i*	*Z*	5.66	10.9	3.60	1740
AlSb	1.6	200	300	*i*	*Z*	6.14	11	4.26	1080
GaP	2.26	300	150	*i*	*Z*	5.45	11.1	4.13	1467
GaAs	1.43	8500	400	*d*	*Z*	5.65	13.2	5.31	1238
GaSb	0.7	5000	1000	*d*	*Z*	6.09	15.7	5.61	712
InP	1.35	4000	100	*d*	*Z*	5.87	12.4	4.79	1070
InAs	0.36	22600	200	*d*	*Z*	6.06	14.6	5.67	943
InSb	0.18	10^5	1700	*d*	*Z*	6.48	17.7	5.78	525
ZnS	3.6	110		*d*	*Z*, *W*	5.409	8.9	4.09	1650†
ZnSe	2.7	600		*d*	*Z*	5.671	9.2	5.65	1100†
ZnTe	2.25		100	*d*	*Z*	6.101	10.4	5.51	1238†
CdS	2.42	250	15	*d*	*W*, *Z*	4.137	8.9	4.82	1475
CdSe	1.73	650		*d*	*W*	4.30	10.2	5.81	1258
CdTe	1.58	1050	100	*d*	*Z*	6.482	10.2	6.20	1098
PbS	0.37	575	200	*i*	*H*	5.936	161	7.6	1119
PbSe	0.27	1000	1000	*i*	*H*	6.147	280	8.73	1081
PbTe	0.29	1600	700	*i*	*H*	6.452	360	8.16	925

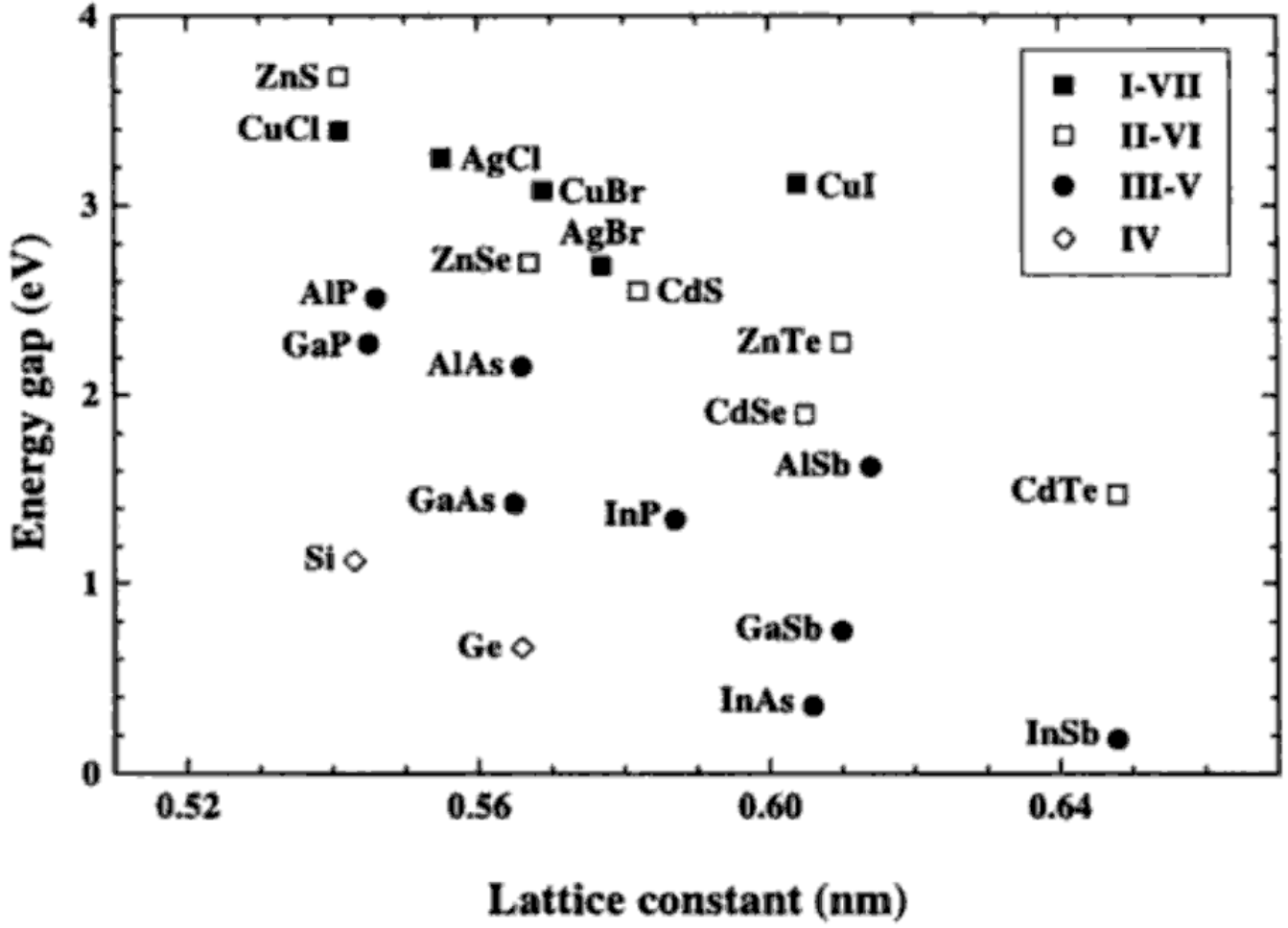

Fig. 1.1. Energy gap vs lattice constant in group IV, III-V, II-VI, and I-VII semiconductors.